# Perceiving slant about a horizontal axis from stereopsis

**Martin S. Banks** Vision Science Program and Department of Psychology, University of California, Berkeley, CA, USA

**Ignace T.C. Hooge** Faculteit Sociale Wetenschappen, Universiteit Utrecht, Utrecht, The Netherlands

**Benjamin T. Backus** Department of Psychology, University of Pennsylvania, Philadelphia, PA, USA

Rotating a surface about a horizontal axis alters the retinal horizontal-shear disparities. Opposed torsional eye movements (cyclovergence) also change horizontal shear. If there were no compensation for the horizontal disparities created by cyclovergence, slant estimates would be erroneous. We asked whether compensation for cyclovergence occurs, and, if it does, whether it occurs by use of an extraretinal cyclovergence signal, by use of vertical-shear disparities, or by use of both signals. In four experiments, we found that compensation is nearly veridical when vertical-shear disparities are available and easily measured. When they are not available or easily measured, no compensation occurs. Thus, the visual system does not seem to use an extraretinal cyclovergence signal in stereoscopic slant estimation. We also looked for evidence of an extraretinal cyclovergence signal in a visual direction task and found none. We calculated the statistical reliabilities of slant-from-disparity and slant-from-texture estimates and found that the more reliable of the two means of estimation varies significantly with distance and slant. Finally, we examined how slant about a horizontal axis might be estimated when the eyes look eccentrically.

Keywords: stereopsis, binocular vision, cyclovergence, surface perception, depth perception

## Introduction

The visual system uses a variety of signals to determine the orientation of a surface. An important signal is provided by the spatial differences in the two eyes' images; the differences are binocular disparities and the resulting percept is stereopsis. Here we examine part of the process of using binocular disparity to determine the orientation of a planar surface.

The orientation of a plane can be represented by its slant and tilt (left side of Figure 1). Slant is the angle between the line of sight to the plane and the surface normal (indicated by the upward arrow); it corresponds with the angle through which the plane is rotated from the frontoparallel plane. Tilt specifies the direction of the rotation. An equivalent representation for tilt refers to the axis about which one would have to rotate a frontoparallel surface in order to make it coplanar with the stimulus. This rotation axis is orthogonal to the tilt; we label it the slant axis in Figure 1. We will use the slant axis to describe tilt because it is more common in the stereopsis literature. Thus, surfaces with a tilt of 0 degree are slanted about a vertical axis and those with a tilt of 90 degees are slanted about a horizontal axis.

The horizontal disparity pattern associated with slant about a vertical axis can be represented locally as a horizontal gradient of horizontal disparity or, alternatively, as a horizontal size ratio (*HSR*), which is the ratio of horizontal angles a surface patch subtends at the left and right eyes (Rogers & Bradshaw, 1993). Changes in *HSR* cause obvious changes in perceived slant, but *HSR* by itself is an ambiguous slant indicator because it is also affected by the plane's position relative to the head (Backus, Banks, van Ee, & Crowell, 1999; Gillam & Lawergren, 1983; Ogle, 1950). Thus, to estimate slant about a vertical axis, the visual system employs other signals to aid the interpretation of horizontal disparity. These signals include vertical disparity (which can be quantified by the vertical size ratio [*VSR*]), eye-position signals (indicating the horizontal version and vergence),

DOI: 10.1167/1.2.1 Received March 23, 2001; Published August 31, 2001 ISSN 1534-7362 © 2001 ARVO

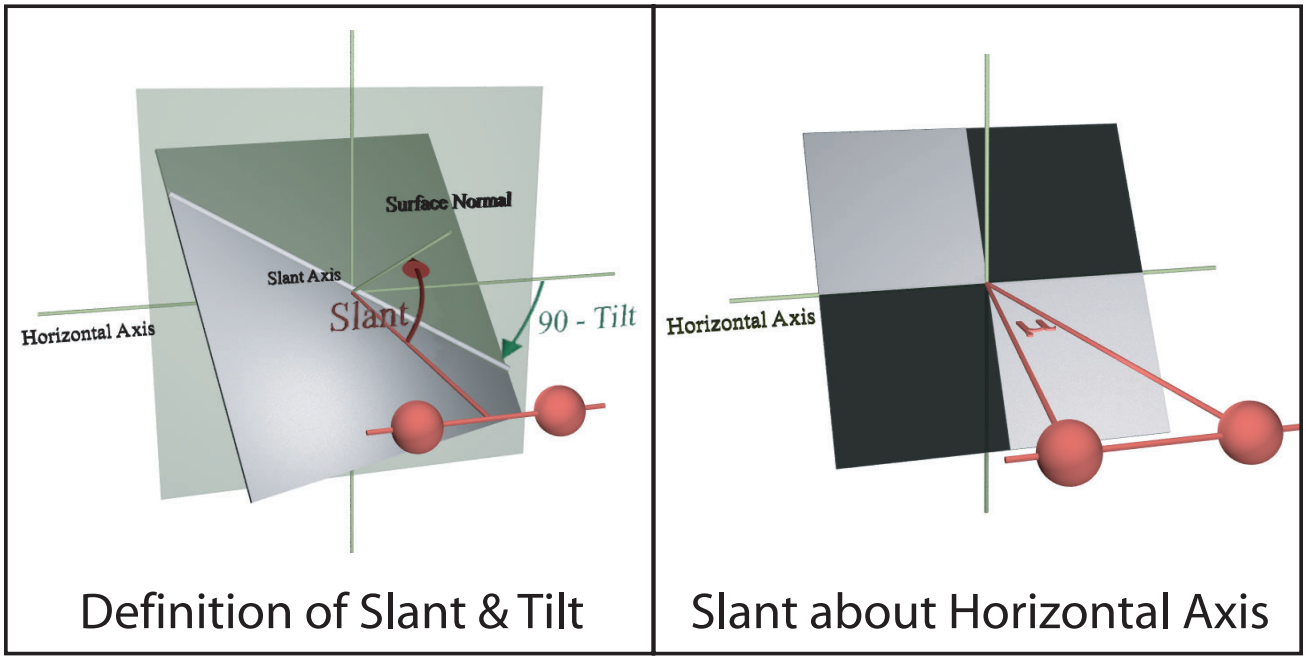


Figure 1. Binocular viewing geometry for estimating surface orientation. Left panel: Definitions of slant and tilt. A binocular observer is viewing a slanted plane. The cyclopean line of sight is represented by the line segment between the midpoint between the eyes and the fixation point, which is the center of the slanted plane. The large green plane is perpendicular to the cyclopean line of sight and represents the gaze-normal plane (for which slant = 0). The gray stimulus plane is rotated with respect to the gaze-normal plane. Slant is the angle between its surface normal and the cyclopean line of sight. Tilt is the angle between the horizontal meridian and the projection of the surface normal. Slant axis is the intersection of the gaze-normal plane and the stimulus plane and corresponds to the axis about which the stimulus plane is rotated relative to the normal plane. Right panel: Slant about a horizontal slant axis; tilt = 90 degrees. The eyes are fixating the middle of the stimulus plane. The eyes' vergence (μ) is the angle between the lines of sight.

and other slant signals, such as the texture gradient (Backus et al, 1999). The horizontal disparity pattern associated with slant about a horizontal axis (right panel of Figure 1) can be represented locally as a horizontal-shear disparity. Ogle and Ellerbrock (1946) defined this disparity as follows. A line through the fixation point and perpendicular to the visual plane is a vertical line. There is a horizontal axis through the fixation point, in the visual plane, and parallel to the interocular axis. We rotate the vertical line about this axis and project the images of the line onto the two eyes. The horizontal-shear disparity ($H_R$) is the angle between the projections of the line in the two eyes. If the eyes are torsionally aligned (ie, the horizontal meridians of the eyes are coplanar) and fixating in the head's median plane, slant about a horizontal axis is given by:

$$S = -\tan^{-1}\left[\frac{\tan(H_R/2)}{\sin(\tan^{-1}(i/2d))}\right] \qquad (1)$$

where $S$ is the slant, $i$ is the interocular distance, and $d$ is the distance to the vertical line's midpoint. When the distance to the surface is much greater than the interocular distance, slant is given to close approximation by:

$$S \approx -\tan^{-1}\left(\frac{1}{\mu}\tan H_R\right) \qquad (2)$$

where μ is the eyes' horizontal vergence (right panel, Figure 1).[1, 2] Thus, estimating slant about a horizontal axis is straightforward when the eyes are aligned: the visual system must only measure the pattern of horizontal disparity (quantified by $H_R$) and the vergence distance (μ), which could also be measured by use of the pattern of vertical disparities (Rogers & Bradshaw, 1995; Backus et al, 1999).

The eyes, however, are not torsionally aligned in all viewing situations. Specifically, the eyes can rotate about the lines of sight; cyclovergence refers to rotations in opposite directions in the two eyes. Let τ represent cyclovergence in Helmholtz coordinates. Intortion ($\tau < 0$; tops of the eyeballs rotated toward one another) occurs with downward gaze at a near target and extorsion ($\tau > 0$) with upward gaze (Somani, DeSouza, Tweed, & Vilis, 1998). Figure 2 illustrates how the resulting torsional misalignment alters the horizontal disparities at the

retinas. In each panel, there is a horizontal-shear disparity created by the stimulus. We will refer to this as $H_S$, a head-centric value, in order to distinguish it from the retinal shear disparity $H_R$. In the upper row, the eyes are torsionally aligned ($\tau = 0$) and are fixating a frontoparallel plane. $H_S$ is 0 near the fixation point. Slant can be recovered from Equations 1 and 2. In the middle row, the eyes are again torsionally aligned, but the plane is now slanted about a horizontal axis ($S < 0$; $H_S > 0$; $\tau = 0$); again slant can be recovered accurately from Equations 1 and 2. In the lower row, the plane is slanted by the same amount as in the middle row, but the eyes are extorted. The shear disparity at the retinas is $H_R = H_S - \tau$. Thus, a particular combination of slant and extortion creates a pattern of horizontal-shear disparity identical to the pattern created by a frontoparallel plane when the eyes are aligned (upper row). If we do not know the torsional state of the eyes, the slant specified by $H_R$ is ambiguous (Ogle & Ellerbrock, 1946; Howard & Kaneko, 1994).

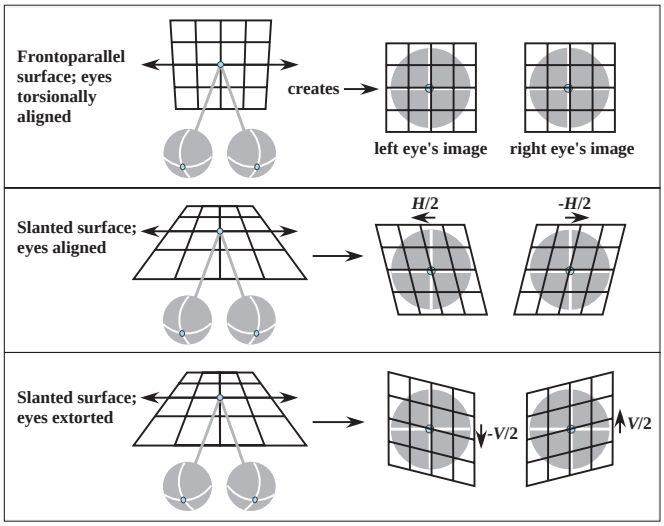


Figure 2. Cyclovergence affects the relationship between slant and horizontal-shear disparity. In each of the three panels, the left side depicts the viewing situation and the right side the shear disparities at the retinas. Upper panel: The observer is viewing a frontoparallel plane with the eyes torsionally aligned ($\tau = 0$). The horizontal-shear disparity is 0. (Note that we have not shown the gradients of vertical disparity that would occur with the viewing of objects at noninfinite distances.) Middle panel: The plane is slanted about a horizontal axis (slant < 0), which creates a positive horizontal-shear disparity. Horizontal-shear disparity is the difference between the orientations of the images of a vertical (right eye minus left eye): $-H_R/2 - H_R/2 = -H_R$. Lower panel: The plane is again slanted about a horizontal axis, but the eyes are also extorted ($\tau > 0$) such that the horizontal-shear disparity is 0. If the visual system did not compensate for the horizontal shear created by cyclovergence, slant would be misestimated.

The need to compensate for changes in the eyes' horizontal vergence and cyclovergence is further illustrated in Figure 3. Each panel shows the slant estimate obtained from Equation 1 as a function of distance (which can be estimated from $\mu$). The horizontal-shear disparity observed at the retinas ($H_R$) is 0, –1, and –2 degrees in the upper, middle, and lower panels, respectively. Each panel shows five curves that correspond to the estimate from Equation 1 for cyclovergences of –4, –2, 0, 2, and 4 degrees. The correct surface slant is indicated by the thick curve in each panel ($\tau = 0$). Estimates obtained from Equation 2 are indicated by the open circles; notice that the estimates are an excellent approximation to the correct estimate for all but very short distances (<10 cm). Clearly, failure to compensate for cyclovergence can have a profound effect on the estimated slant; for example, at a distance of 100 cm, the estimation error is –47.5, –28.6, 0, 28.6, and 47.5 degrees for cyclovergences of 4, 2, 0, –2, and –4 degrees, respectively. Likewise, failure to compensate for changes in horizontal vergence (correlate of distance) can have a large effect on the slant estimate; for example, when $H_R$ = –2 degrees (lower panel) and the eyes are torsionally aligned ($\tau = 0$), the correct slant varies from ~0 degree at very near distances to 47.5 degrees at 200 cm. Here we ask whether the visual system compensates for changes in cyclovergence and horizontal vergence and, if it does compensate, the means by which the compensation is accomplished.

The visual system could in principle compensate for cyclovergence and horizontal vergence by use of extraretinal signals. In particular,

$$S \approx -\tan^{-1}\left[\frac{1}{\mu}\tan(H_R + \hat{\tau})\right] \qquad (3)$$

where $\hat{\tau}$ is an extraretinal cyclovergence signal and $\mu$ is the horizontal vergence and could be measured by an extraretinal vergence signal. If the extraretinal cyclovergence signal is accurate, $\hat{\tau} = \tau$. To our knowledge, there is no evidence that an extraretinal torsion signal exists,[3] but the possibility should be entertained because it has been shown that extraretinal signals of horizontal version and horizontal vergence are used in interpreting horizontal disparity patterns (Backus, et al, 1999; Rogers & Bradshaw, 1995).

The visual system could also compensate for cyclovergence by use of vertical-shear disparity. Cyclovergence and slant about a horizontal axis produce different effects on the retinal images; specifically, cyclovergence alters the pattern of vertical disparities at the horizontal meridians of the eyes, but horizontal-axis slant changes do not (Rogers, 1992; Howard, Ohmi, & Sun, 1993; Howard & Kaneko, 1994). This is illustrated in the middle and lower panels of Figure 2.

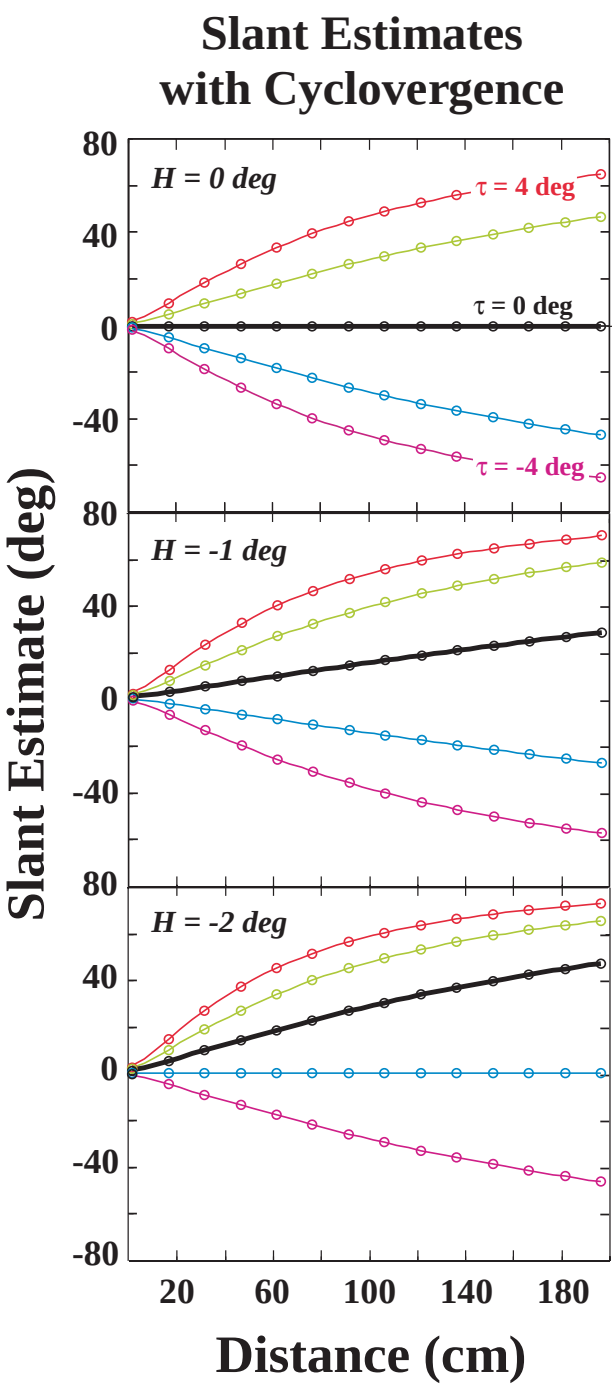


Figure 3. Slant estimates as a function of distance, slant, and cyclovergence. Each panel plots the slant estimate as a function of distance for a given horizontal-shear disparity ($H_R$). The upper, middle, and lower panels show the estimates when $H_R$ = 0, –1, and –2 degrees, respectively. The true slant in each panel is indicated by the black curve. The five curves in each panel represent the estimates when the cyclovergence ($\tau$) is –4, –2, 0, 2, and 4 degrees. The slant estimates derived from Equation 1 are indicated by the thin colored curves and the estimates derived from Equation 2 by the small circles. Equation 2 provides an excellent approximation to Equation 1. It is important to note the large errors in slant estimation that would occur if there were no compensation for the effects of cyclovergence.

Vertical-shear disparity ($V_R$) can be defined as the angle between the projections of a horizontal line in the two eyes (lower panel, Figure 2). Slant about the horizontal axis is given to close approximation by

$$S \approx -\tan^{-1}[\frac{1}{\mu}\tan(H_R - V_R)]. \qquad (4)$$

So the visual system could, in principle, estimate slant even when the eyes are torsionally misaligned by measuring $H_R$, $V_R$, and distance. This equation predicts that changes in perceived slant can be induced by altering $H_R$ or $V_R$, and such an effect has been demonstrated by Ogle and Ellerbrock (1946), Howard and Kaneko (1994), and others.

There is, of course, a variety of monocular slant signals that can be used to estimate slant about a horizontal axis. The most obvious such signal is the texture gradient, which can be used to estimate surface slant and tilt (Gibson, 1950; Knill, 1998a). The utility of the texture gradient is unaffected by cyclovergence and horizontal vergence, so the visual system would not have to compensate for vergence changes when using this slant signal to estimate local surface orientation. We were able to eliminate the influence of these signals in the work presented here, so we focus only on disparity and extraretinal signals.

There is clear experimental evidence that the visual system can use both extraretinal signals and patterns of vertical disparity to compensate for changes in horizontal vergence. Thus, we will focus here on cyclovergence. There are three possible means of compensation.

1. Perhaps compensation does not occur, so cyclovergence changes lead to errors in slant estimation such as those shown in Figure 3. We will refer to this as the *no-compensation* model. It is represented quantitatively by Equations 1 and 2.
2. Perhaps compensation occurs via use of an extraretinal torsion signal. We will refer to this as the *extraretinal-compensation* model. It is represented quantitatively by Equation 3.
3. Perhaps compensation occurs via use of vertical-shear disparity. We will refer to this as the *vertical-disparity-compensation* model. It is represented by Equation 4.

Several investigators have examined the stereoscopic estimation of slant about a horizontal axis (Ogle & Ellerbrock, 1946; Gillam & Rogers, 1991; Howard & Kaneko, 1994; Kaneko & Howard, 1997; Howard & Pierce, 1998; Pierce, Howard, & Feresin, 1998; van Ee & Erkelens, 1998). For example, Howard and Kaneko (1994) showed that the introduction of vertical-shear disparity causes a surface to appear slanted in the direction predicted by Equation 4.

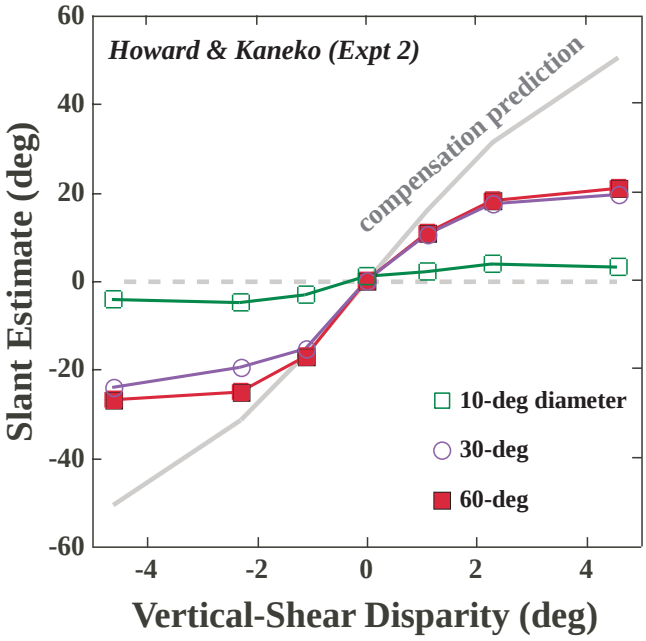


Figure 4. The data of Howard and Kaneko (1994). Observers' slant estimates are plotted as a function of vertical-shear disparity. Howard and Kaneko did not measure cyclovergence, so vertical shear refers to its head-centric value ($V_S$). The dashed line at 0 indicates the expected slant estimates if vertical-shear disparity did not affect perceived slant. The solid curve indicates the expected estimates if vertical shear were used veridically in the manner suggested by Equation 4. The data points represent the observers' average slant estimates: unfilled squares, circles, and filled squares are the data for stimulus diameters of 10, 30, and 60 degrees, respectively.

Figure 4 shows the data from their first experiment. Perceived slant is plotted as a function of vertical-shear disparity; we refer to this as $V_S$, which is a head-centric disparity, to distinguish it from $V_R$, which is a retinal disparity. The solid gray curve is the predicted slant according to the vertical-disparity-compensation model (Equation 4). The data fell short of the prediction. For three reasons, we cannot determine from these data (nor from the data of the other reports listed above) precisely how the visual system compensates for cyclovergence. First, Howard and Kaneko,1994,(and the others listed above) did not measure the eyes' cyclovergence during the experimental measurements. Vertical-shear disparity is known to stimulate cyclovergence (Rogers, 1992), so it is quite likely that cyclovergence covaried with vertical shear in this experiment. Thus, one cannot determine from these data how much of the observed compensation was due to vertical-disparity as opposed to extraretinal compensation. Second, the stimulus in the Howard and Kaneko experiment (and the others listed above) contained monocular slant signals (texture gradient and outline shape) and those signals always specified a slant of 0. Human observers take both monocular and stereoscopic estimates into account when judging surface slant (Buckley & Frisby, 1993; Banks & Backus, 1998), so Howard and Kaneko's data are almost certainly contaminated by monocular slant signals. Third, Howard and Kaneko asked observers to adjust a paddle with the unseen hand until it was judged to have the same slant as the visual stimulus (others used a variety of estimation techniques). To do this, the observer has to convert the internal slant estimate into a manual response. The problem is that we do not know the function that maps internal estimate into response, so we cannot determine how much of the prediction shortfall was caused by this mapping function.

We were able to circumvent these three problems and thereby determine quantitatively the means by which the visual system takes cyclovergence into account.

# General Methods

## Observers

The three authors participated in the experiments. M.S.B. and I.T.H. have normal vision. B.T.B. is a 7-diopter myope and wore correcting contact lenses during the experimental measurements.

## Apparatus

Stimuli were displayed on a haploscope consisting of two 58-cm monochrome cathode-ray tubes (CRT), one seen by the left eye in a mirror placed near that eye and the other seen by the right eye in a mirror placed near that eye. Each mirror and CRT was attached to an armature that rotated about a vertical axis. The observer was positioned such that the rotation axes of the two armatures were co-linear with the vertical rotation axes of the eyes. A custom sighting device was used for this positioning (Hillis & Banks, 2001). When adjusted correctly, head position was fixed with a bite bar. Natural pupils were used. The distance to the CRTs was fixed at 42 cm. The room was completely dark except for the white dots and lines in the stimuli.

A Macintosh 840/AV generated the stimuli and collected the responses. Each CRT displayed 1280 x 1024 pixels at a refresh rate of 75 Hz. Angular subtense of a pixel was ~2.5 minarc at screen center. Despite the short viewing distance, the visual locations of the dots and lines in our displays were specified to within ~30 arcsec. This high level of spatial precision was achieved by anti-aliasing and spatial calibration (Backus et al, 1999).

# Experiment 1: Slant Estimation During Natural Viewing

We first asked whether observers compensate for changes in cyclovergence when judging surface slant about a horizontal axis. To do so, we induced cyclovergence of different amounts and then flashed a large random-dot plane. Observers adjusted the plane's slant about a horizontal axis until it appeared perpendicular to the line of sight. The stimulus and procedure were designed so that the task had to be performed from disparity and eye-position signals alone (Equations 1-4) and was uncontaminated by monocular slant signals.

## Method

The conditioning stimulus, nonius stimulus, and test stimulus used in this experiment are depicted in Figure 5.

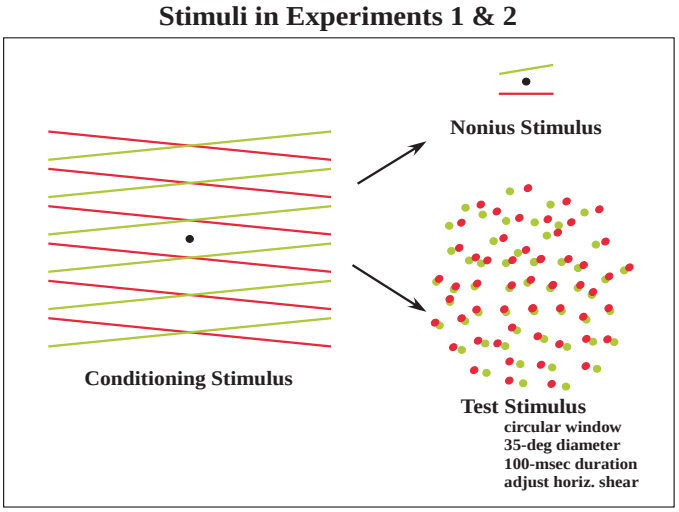


Figure 5. Stimuli and procedure in Experiments 1 and 2. The red lines and dots represent stimuli presented to the right eye, and the green lines and dots represent stimuli presented to the left eye. The procedure and conditioning, nonius, and test stimuli are described in the text.

### *Conditioning Stimulus*

The conditioning stimulus was used to induce cyclovergence. The stimulus was a large (35 x 35 degrees) field of horizontal lines. The lines were rotated about the lines of sight in opposite directions in the two eyes (Figure 5). The cyclorotation values were –4, –2, 0, 2, or 4 degrees; different cyclorotation values were presented in different experimental sessions. During presentation of this conditioning stimulus, observers maintained fixation on a small central dot seen by both eyes.

Cyclovergence to a cyclorotated stimulus is typically slow (Howard & Zacher, 1991). Indeed, we observed that the maximum response to the larger cyclodisparities could occur 2 to 4 minutes after the beginning of the session. Because our adjustment procedure involved numerous stimulus presentations, cyclovergence reached a constant state before the final slant settings were made.

### *Nonius Stimulus*

The nonius stimulus was used to measure the eyes' cyclovergence while the observer performed the experimental task. It consisted of two 4-degree line segments. One segment was positioned one-half degree above the central fixation dot and was presented to the left eye and the other was one-half degree below the dot and was presented to the right eye. The stimulus was flashed for 100 msec and the observer indicated with a key press whether the upper line appeared rotated clockwise or counter-clockwise with respect to the lower line. The orientation difference required to make the lines appear parallel was the measure of cyclovergence.[4] We confirmed in another experiment that this subjective technique is an accurate and reliable measure of cyclovergence (Hooge, Banks, & van den Berg, 2001).

### *Test Stimulus*

The test stimuli were sparse random-dot displays simulating planes of different slants about a horizontal axis. The dots were randomly distributed within a circle subtending 35 degrees at the cyclopean eye. There were approximately 300 dots in each stimulus.

Because we were interested in examining stereoscopic slant estimation only, we designed a stimulus and procedure that eliminates contamination by monocular slant signals. The outline shape of the stimulus (at the cyclopean eye) was circular for all slants, so it always specified a slant of 0 degree. The dot distribution was determined using a back-projection technique (Banks & Backus, 1998), so the texture gradient also specified a constant slant of 0 degree. The key element, however, is the use of a slant-nulling procedure: observers adjusted the horizontal-shear disparity in the stimulus until the resulting percept was a gaze-normal plane. Because the monocular slant signals always specified a slant of 0,[5] any adjustment made by the observer had to be based on disparity signals specifying a slant other than 0.

### *Procedure*

Our experimental procedure was designed so that we could know the eyes' cyclovergence when the observer performed the slant-nulling task. Each experimental session began with a particular conditioning stimulus (–4 to 4 degrees cyclorotation). It was initially presented for 10 sec while the observer maintained fixation on the central fixation dot. The conditioning stimulus was then replaced for 100 msec by the nonius stimulus. The observer indicated whether the upper line appeared rotated clockwise or counter-clockwise with respect to the

lower line. The conditioning stimulus reappeared for 2 sec and was then replaced for 100 msec by the test stimulus.[6] The observer indicated whether the top of the test plane appeared slanted forward or backward. The conditioning stimulus reappeared for 2 sec and the whole procedure was repeated. The observer adjusted the nonius lines and the test stimulus with large initial steps and then progressively smaller steps. He always made enough adjustments to make sure that the direction of change had reversed at least four times. When the observer was satisfied with *both* settings, he indicated this with a key press and a new stimulus sequence was begun.

There were five experimental conditions (–4, –2, 0, 2, and 4 degrees cyclorotation). Several adjustments were made in each of the five conditions before beginning another condition.

## Results and Discussion

The conditioning stimulus induced significant cyclovergence, but response gain was significantly less than 1. Figure 6 plots the observed cyclovergence (measured with the nonius technique and confirmed by objective recording; Hooge et al, 2001) as a function of the cyclorotation stimulus. The dashed line indicates the expected cyclovergence if the gain were 1. The data points and solid lines indicate the observed responses of the three observers. The gains were 0.55, 0.73, and 0.24 in I.T.H., B.T.B., and M.S.B., respectively. These values are similar to those reported in the literature (Howard & Zacher, 1991).

Figures 7 and 8 show the data from the slant-nulling task. The horizontal-shear disparity at the retinas ($H_R$) of the observers' settings is plotted as a function of the eyes' cyclovergence. To determine the retinal disparity ($H_R$), we subtracted the measured cyclovergence for the appropriate condition from the head-centric horizontal shear at the CRTs ($H_S$). If observers failed to compensate for changes in cyclovergence, the data would be independent of the eyes' torsion and would fall on a horizontal line at $H_R = 0$. On the other hand, if observers compensated for cyclovergence in the fashion suggested by Equation 3 (extraretinal compensation with an accurate torsion signal) or by Equation 4 (vertical-disparity compensation), the data would fall on the diagonal line (along which $H_R = -\tau$).

Figure 7 shows the individual settings by observer I.T.H., and Figure 8 shows the average settings (averaged horizontally for cyclovergence and vertically for shear disparity[7]) by I.T.H., B.T.B., and M.S.B. All the data suggest that observers compensated for changes in cyclovergence and estimated slant nearly veridically.

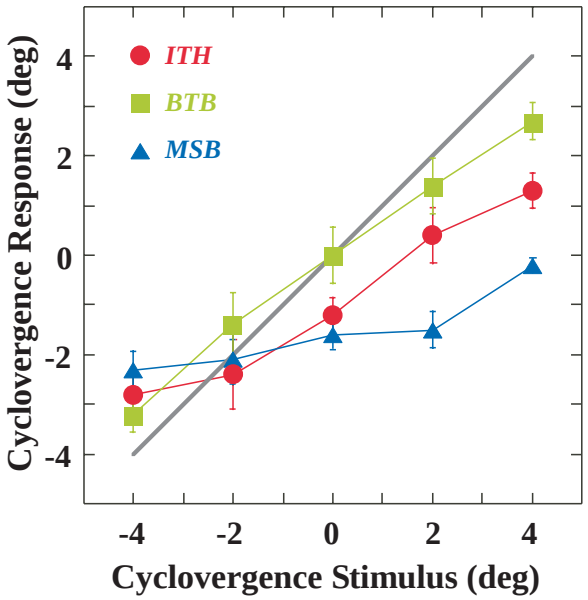


Figure 6. Cyclovergence as a function of the cyclodisparity presented in the conditioning stimulus. The cyclovergence response was determined using the nonius technique. The gray diagonal line represents the expected response if the gain of cyclovergence was 1. The data points represent the observed responses of our three observers. Error bars represent ±1 SD.

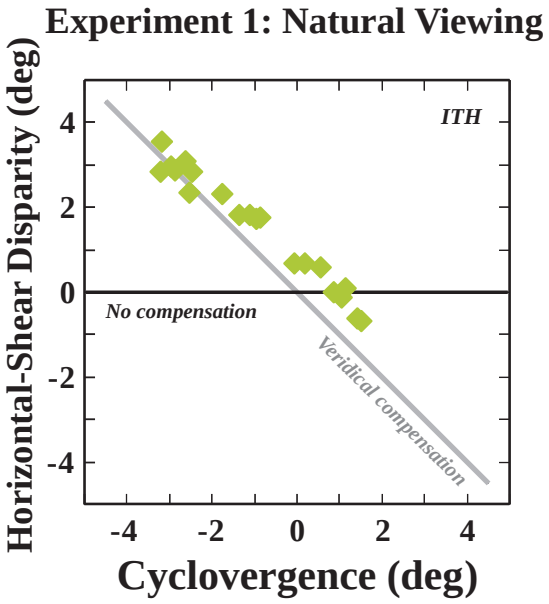


Figure 7. Experiment 1 results for observer I.T.H. The horizontal-shear disparity that appeared gaze normal is plotted as a function of the eyes' cyclovergence (measured with the nonius technique). The horizontal shear is in retinal coordinates. The vertical-shear disparity was always 0 (in head-centric coordinates), so any vertical shear at the retinas was caused by cyclovergence. If no compensation for cyclovergence occurred, the data would lie on the horizontal line. If veridical compensation occurred, the data would lie on the diagonal line. Each data point represents a single setting.

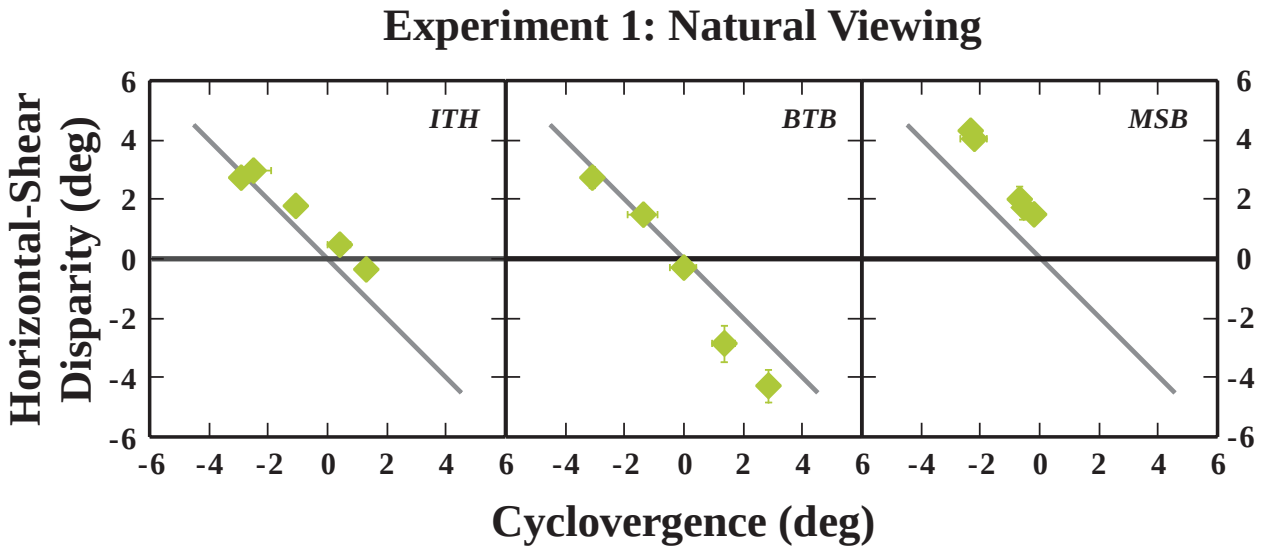


Figure 8. Average results from Experiment 1. The horizontal-shear disparity that appeared gaze normal is plotted as a function of the eyes' cyclovergence. Horizontal shear is in retinal coordinates. If no compensation for cyclovergence occurred, the data would lie on the horizontal lines. If veridical compensation occurred, the data would lie on the diagonal lines. Each panel shows the average settings from one of the three observers. The averages were done on the settings for each of the conditioning stimuli. Error bars represent ±1 SD.

## Experiment 2: Extraretinal or Vertical-Disparity Compensation?

We next investigated the means by which the visual system compensates for changes in cyclovergence. We did so by independently varying the vertical-shear disparity in the stimulus while inducing different amounts of cyclovergence. The stimulus was again devoid of informative monocular slant signals, so the task had to be performed from the disparity and eye-position signals alone.

### Method

The stimuli and procedure were identical to those in Experiment 1 with one exception: the test stimulus contained different amounts of vertical-shear disparity ($V_S$). Specifically, vertical-shear disparities of –4, –2, 0, 2, or 4 degrees (head-centric coordinates) were added to the random-dot test stimulus. The vertical-shear disparity at the retinas was, therefore, the difference between the added vertical shear and the disparity created by the eyes' cyclovergence: $V_R = V_S - \tau$.

### Results and Discussion

The conditioning stimulus again induced significant cyclovergence, and again response gain was less than 1.

Figures 9 and 10 show the data from the slant-nulling task. Again the retinal horizontal-shear disparity ($H_R$) of the observers' settings is plotted as a function of the eyes' cyclovergence. If observers failed to compensate for changes in cyclovergence, the data would fall on the horizontal line at $H_R = 0$. If observers compensated for cyclovergence by use of an extraretinal torsion signal (Equation 3), then only the horizontal-shear disparity and the eyes' torsional state would matter. In this case, the data would fall on the middle diagonal line. Finally, if observers compensated for cyclovergence by use of the added vertical-shear disparity (Equation 4), then only the horizontal and vertical-shear disparities at the retinas would matter. Specifically, a slant of zero would be perceived whenever the vertical and horizontal shears were equal to one another. The data would fall on the series of diagonal lines, a different line for each added vertical-shear disparity ($V_S$).

Figure 9 displays the individual settings by observer I.T.H. and Figure 10 displays the average settings (averaged horizontally for cyclovergence and vertically for horizontal-shear disparity) by I.T.H., B.T.B., and M.S.B. The data are clearly most consistent with the predictions of Equation 4. In other words, observers' settings were more consistent with the predictions of the vertical-disparity compensation model than with the other models. This result is consistent with the conclusions

drawn by Howard and Kaneko (1994), Kaneko and Howard (1997), Allison, Howard, Rogers, & Bridge (1998), Howard and Pierce (1998), Pierce et al (1998), and van Ee and Erkelens (1998).

The vertical-disparity model predicts a larger effect of added vertical-shear disparity than we actually observed. For example, consider the data for a cyclovergence value of 0 degree. For I.T.H., the average settings for vertical shears of –4 to 4 degrees ranged from approximately –2.5 to 3.2 degrees. For B.T.B., the settings ranged from approximately –5 to 3.2 degrees, and for M.S.B., they ranged from –0.5 to 4 degrees. We can express these as gains: specifically, the range of horizontal shears at the null settings divided by the range of vertical shears. The gains for I.T.H., B.T.B., and M.S.B. were 0.71, 0.97, and 0.56, respectively. Does this mean that the visual system does not fully implement compensation based on vertical-shear disparity? The answer is, not necessarily, because the proposed extraretinal compensation mechanism predicts that the data should fall on the middle diagonal line.

Thus, the shortfall we observed could be due to conflicting information arising from the extraretinal compensation. The next 2 experiments were designed to test this possibility.

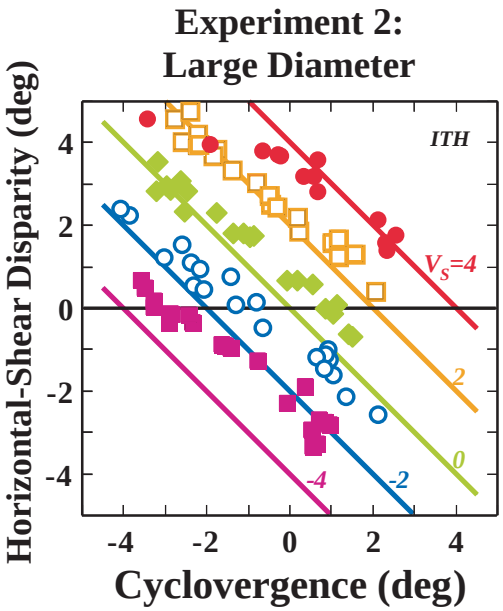


Figure 9. Experiment 2 results for observer I.T.H. The horizontal-shear disparity that appeared gaze normal is plotted as a function of cyclovergence. Horizontal shear is in retinal coordinates. Stimulus diameter was 35 degrees. Vertical-shear disparity (in head-centric coordinates) was –4, –2, 0, 2, or 4 degrees; each is represented by a different data symbol. Vertical shear at the retinas was the sum of the vertical shear added to the stimulus plus the effect of cyclovergence. If no compensation for cyclovergence occurred, the data would lie on the horizontal line. If veridical compensation based on use of vertical-shear disparity occurred (Equation 4), the data would lie on the diagonal lines. If veridical compensation based on use of an extraretinal, cyclovergence signal occurred (Equation 3), the data would lie on the central diagonal line. Each data point represents 1 setting.

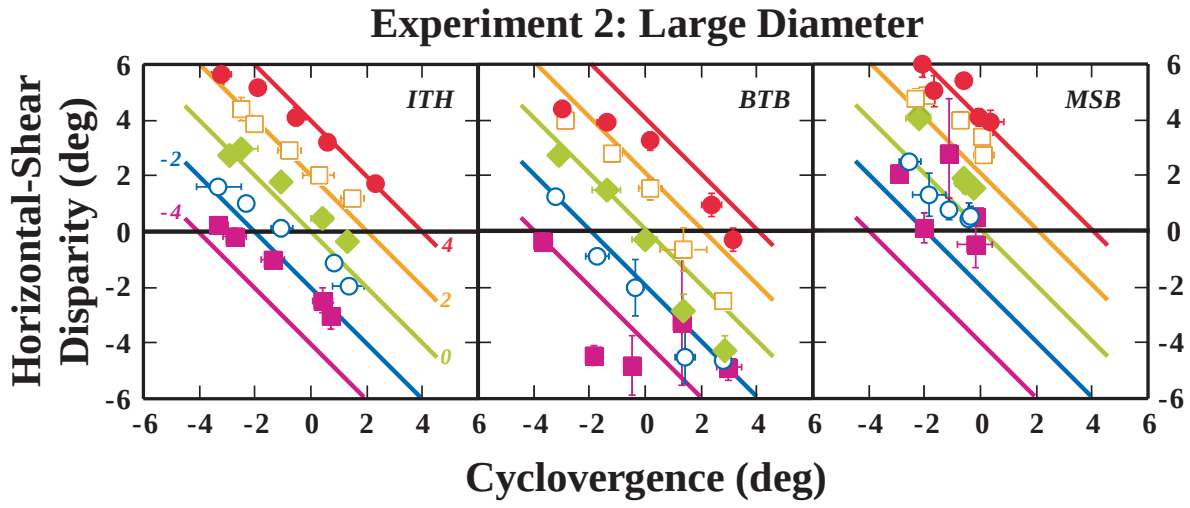


Figure 10. Average results from Experiment 2. The retinal horizontal-shear disparity that appeared gaze normal is plotted as a function of cyclovergence. Stimulus diameter was 35 degrees. The vertical-shear disparity (in head-centric coordinates) was –4, –2, 0, 2, or 4 degrees; each case is represented by a different data symbol. The predictions are the same as in Figure 9. Each panel shows the average settings from one of the three observers. The averages were done on the settings for each of the conditioning stimuli. Error bars represent represents ±1 SD.

## Experiment 3: Compensation When the Stimulus Is Small

One can distinguish between the value of a signal and the ease with which that value can be measured by the visual system. A signal such as vertical shear becomes difficult to measure in a small image: with less area across which to average, local noise becomes relatively more significant. In Experiment 3, we decreased stimulus diameter and again independently varied the vertical-shear disparity in the stimulus while inducing different amounts of cyclovergence. The idea was not to change the value of the vertical shear signal, but to render it difficult to measure. We could then look for manifestations of extraretinal compensation because the visual system would be expected to rely more heavily on extraretinal signals when the alternative method (vertical shear) is unreliable. This strategy was used successfully by Rogers and Bradshaw (1995) (for horizontal vergence and curvature estimation) and by Backus et al (1999) (for horizontal version and estimating slant about a vertical axis).

### Method

The stimuli and procedure were identical to those of Experiment 2 except stimulus diameter was reduced from 35 to 5 degrees. Dot number was decreased to hold dot density roughly constant.

### Results and Discussion

Figures 11 and 12 show the data. Retinal horizontal-shear disparity ($H_R$) of the observers' settings is plotted as a function of the eyes' cyclovergence. If observers failed to compensate for changes in cyclovergence, the data would fall on the horizontal line at $H_R = 0$. If they compensated for cyclovergence by use of an extraretinal torsion signal (Equation 3), the data would fall on the middle (green) diagonal line. We assume that the vertical-shear disparity cannot be measured reliably with the stimulus used in this experiment, so compensation by vertical disparity is unlikely.

Figure 11 shows the individual settings by observer I.T.H. and Figure 12 shows the average settings by I.T.H., B.T.B., and M.S.B. As before, the different symbols represent different added vertical-shear disparities. The predictions are the same as in Figures 9 and 10: the horizontal line at $H_R = 0$ is the prediction for no compensation, the five diagonal lines are the predictions for vertical-disparity compensation, and the middle (green) diagonal line is the prediction for extraretinal compensation. We conducted an analysis of variance on the data in Figure 12: there was no significant effect of vertical-shear disparity on any of the three observers' data. Because there was no systematic effect of vertical-shear disparity, we conclude that observers were indeed unable to use this signal when it was made smaller. This specific finding is consistent with the results of Howard and Kaneko's (1994) second experiment (see their Figure 4). The data also appear to be inconsistent with the prediction for extraretinal compensation. The analysis of variance revealed no significant effect of the eyes' cyclovergence with the exception of observer B.T.B. who showed a small effect: $P < 0.01$ (notice that the slope of B.T.B.'s data is much less than the slope of the extraretinal prediction, so his compensation was far short of veridical). Overall, the data are most consistent with a failure to compensate for changes in cyclovergence.

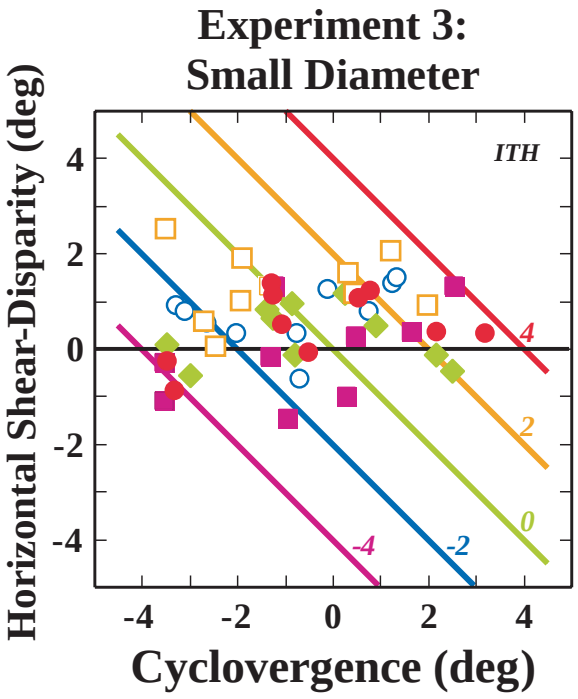


Figure 11. Experiment 3 results for observer I.T.H. The retinal horizontal-shear disparity that appeared gaze normal is plotted as a function of cyclovergence. Stimulus diameter was 5 degrees. The vertical-shear disparity (in head-centric coordinates) was –4, –2, 0, 2, or 4 degrees; each case is represented by a different data symbol. The predictions are the same as in Figure 9. Each data point represents 1 setting.

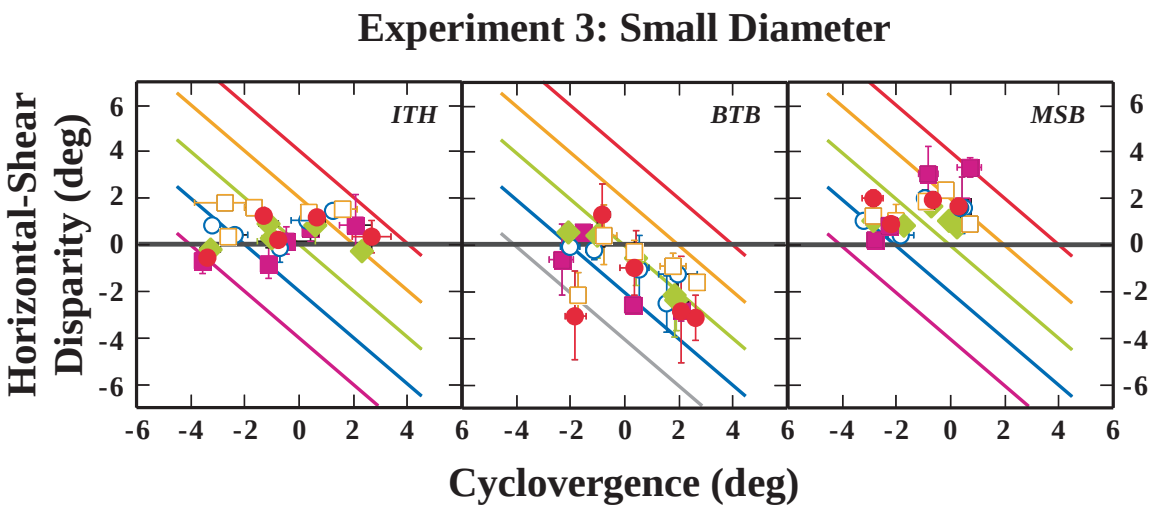


Figure 12. Average results from Experiment 3. The retinal horizontal-shear disparity that appeared gaze normal is plotted as a function of the eyes' cyclovergence. Stimulus diameter was 5 degrees. Each vertical-shear disparity is represented by a different data symbol. The predictions are the same as in Figure 9. Each panel shows the average settings from one of the three observers. The averages were done on the settings for each of the conditioning stimuli. Error bars represent ±1 SD.

When the induced vertical-shear disparity is difficult to measure, human observers apparently fail to compensate for changes in cyclovergence. We found little evidence for compensation by means of an extraretinal torsion signal. This means that the perceived slant of a small surface changes when the eyes make torsional movements in opposite directions.

## Experiment 4: Compensation When Vertical Disparities Are Unmeasurable

In Experiment 3, the test stimulus contained small vertical disparities, so they were presumably an unreliable source of information. The conditioning stimulus, however, provided a clear vertical disparity signal. It is possible that the vertical disparity signal from the conditioning stimulus persisted through the test stimulus interval and thereby affected the perceived slant of the test stimulus. We know little about the temporal properties of vertical-disparity compensation (Allison et al, 1998), so we cannot reject this hypothesis. As a consequence, we designed an experiment in which cyclovergence changed without use of a conditioning stimulus. Specifically, we tried to use a feature of natural binocular eye movements to create the desired cyclovergence changes.

Listing's Law describes the manner in which the eyes rotate from primary position (gazing straight ahead at infinity) to other distant positions; the eyes rotate such that the axis of rotation lies in a plane parallel to the forehead (Howard & Rogers, 1995). It was thought that Listing's Law did not hold for fixation of near targets because the eyes rotate about the lines of sight during horizontal vergence. It has been discovered more recently that eye rotations to fixate near targets still occur about axes confined to a plane, but the planes are rotated temporally. Seen from above, the left eye's plane is rotated counter-clockwise and the right eye's plane clockwise. Listing's Extended Law states that each plane is rotated by one half of the horizontal vergence ($\mu/2$) (Somani et al, 1998; Tweed, 1997). To understand the consequence of Listing's Extended Law, consider an observer looking at a gaze-normal surface consisting of a cross. The observer pitches the head upward or downward while maintaining fixation on the cross. According to Listing's Extended Law, the eyes will move such that the vertical and horizontal limbs of the cross will continue to fall on the eyes' vertical and horizontal meridians. Said another way, no horizontal- or vertical-shear disparity will be introduced as the observer pitches the head. Measurements of binocular eye movements reveal that not all observers follow Listing's Extended Law (Somani et al, 1998); in upward gaze of near targets those observers tend to have the eyes extorted relative to prediction and in downward gaze they tend to have the eyes intorted relative to prediction. We used this to create changes in cyclovergence without presenting a vertical-shear stimulus.

### Method

The stimuli and procedure were the same as in the previous experiments with two notable exceptions. First, cyclovergence was varied by having observers fixate a near

target while looking down, straight ahead, or up. Second, the test stimulus consisted of a smooth vertical line so that vertical disparity could not be measured.

In order to allow downward and upward gaze, we modified the bitebar mount in the haploscope. The mount was attached to a yoke that allowed us to pitch the observer's head upward or downward about the interocular axis. When the observer's head was pitched upward, he had to look downward to maintain gaze on the fixation point. Similarly, with downward head pitch, he had to look upward to maintain fixation. Three head-pitch conditions were presented: 20 degrees up, straight ahead, and 20 degrees down. The distance to the fixation point (and test stimulus) was set such that the horizontal vergence angle was 18.7 degrees. With this technique we hoped to create extorsion with upward gaze and intorsion with downward gaze. As before, we used the nonius stimulus to measure the eyes' actual cyclovergence.

The test stimulus consisted of a smooth vertical line 40 degrees in height. Vertical disparity could not be measured on the line because there were no discernible features to match between the two eyes. (The tops and bottoms of the line were clipped at random positions in the two eyes as well.) The observer's task was to adjust the slant of the test line (by altering its horizontal-shear disparity) until the line appeared gaze normal.

As before, the procedure involved adjusting the nonius and test stimuli separately until the observer was satisfied with both settings. The duration of both stimuli was 100 msec so they would not serve as a stimulus to cyclovergence. A binocular dot in the middle of the display served as the fixation guide during presentation of the nonius and test stimuli and in-between those presentations.

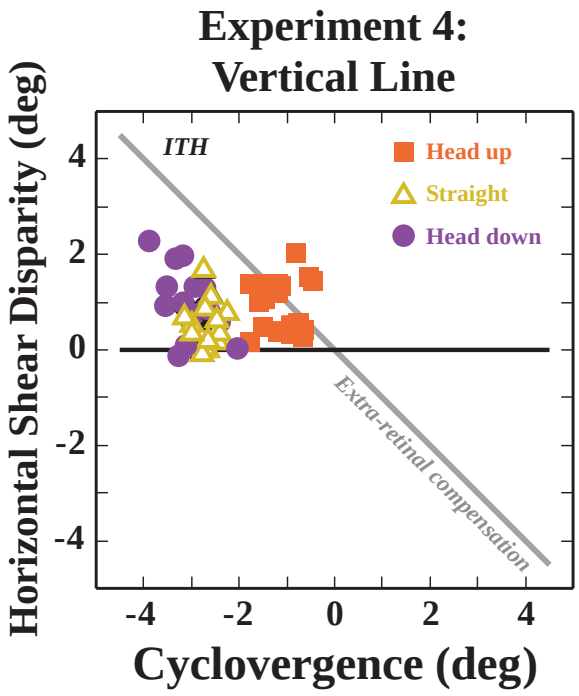


Figure 13. Experiment 4 results for observer I.T.H. The retinal horizontal-shear disparity that appeared gaze normal is plotted as a function of the eyes' cyclovergence (measured with the nonius technique). The stimulus was a 40-degrees tall vertical line. Cyclovergence was created by having the observer pitch the head up or down 20 degrees while fixating at near (vergence = 18.7 degrees). If no compensation occurred, the data would lie on the horizontal line. If veridical compensation via an extraretinal signal occurred, the data would lie on the diagonal line. Each data point represents 1 setting. The red squares are the data when the head was pitched up (eyes down), the green triangles when the head was upright (eyes straight ahead), and the blue circles when the head was pitched down (eyes up).

## Results and Discussion

Two of the three observers (M.S.B. and B.T.B.) followed Listing's Extended Law fairly accurately, so pitching the head up and down did not create cyclorotation of a gaze-normal stimulus. However, observer I.T.H. failed to follow the Extended Law, so head pitch caused reasonably systematic changes in cyclorotation with changes in gaze elevation: on average it was –3.3 degrees with upward gaze, –2.7 degrees with forward gaze, and –1.3 degrees with downward gaze. Figure 13 shows the individual settings by observer I.T.H. The retinal horizontal-shear disparity of the stimulus when it appeared gaze normal is plotted as a function of the eyes' cyclovergence. The different symbols represent the data for upward, straight, and downward gaze. The horizontal line at $H_R = 0$ is the prediction for no compensation and the diagonal line is the prediction for extraretinal compensation. For the purposes of determining whether compensation occurred, we are looking for an effect of head pitch on the disparity setting. The vertical position of the data points is unimportant because it is affected by the observer's criterion for what constitutes a slant of 0. The figure shows that there was no systematic effect of the eyes' cyclovergence. An analysis of variance was conducted on the data and revealed no significant effect of cyclovergence. Thus, the data are most consistent with the no-compensation model. When vertical-shear disparity is unmeasurable (in the test stimulus and in preceding stimuli), there appears to be no compensation for the eyes' torsional state.

Our data are limited because two of the three observers did not exhibit sufficient changes in cyclovergence, but the data from the remaining observer suggest that compensation via the hypothesized extraretinal torsion signal does not occur. This does not necessarily mean that such an extraretinal signal does not exist. Rather it means that such a signal is not used when estimating the slant of a surface stereoscopically.

# General Discussion

We examined the means by which slant about a horizontal axis is estimated from stereoscopic stimuli. The problem is interesting because eye torsions cause a change in horizontal disparity and, if the visual system failed to compensate for this change, large errors in slant estimation would occur. We found that the visual system does compensate for cyclovergence eye movements. It does so by using the vertical-shear disparity that is created by cyclovergence to "correct" the measured horizontal-shear disparity; this result agrees qualitatively with previous reports of Ogle and Ellerbrock (1946), Howard and Kaneko (1994), and others. We found no evidence for use of an extraretinal, cyclovergence signal in the compensation process.

In the discussion, we take up several issues related to these observations. First, having found no evidence for use of an extraretinal, cyclovergence signal, we ask whether such a signal can be demonstrated in other binocular phenomena. Second, we investigate the reliability of stereoscopic and nonstereoscopic slant signals. Third, we investigate why we found nearly veridical compensation via vertical disparity while others found much less compensation. Fourth, we show how the forgotten paper of Ogle and Ellerbrock (1946) illustrates the efficient use of vertical-shear disparity in the compensation process. Fifth, we investigate how slant about a horizontal axis might be estimated when the eyes look eccentrically (eg, left and right, up and down) and discuss the phenomenon of slant anisotropy.

## Is There an Extraretinal Cyclovergence Signal?

We found in Experiments 3 and 4 that reducing or eliminating the usefulness of vertical disparity signals led to a failure to compensate for cyclovergence. Said another way, when the eyes were in different cyclovergence states, the visual system accepted the same horizontal-shear disparity at the retinas as gaze normal. This shows that compensation via an extraretinal cyclovergence signal does not occur in the interpretation of disparity. We wondered if other binocular phenomena would manifest such an extraretinal signal.[8]

Perceived visual direction is clearly affected by extraretinal signals associated with horizontal and vertical eye movements. Hering (1868) observed, for example, that an afterimage appears to move leftward and rightward with horizontal versions and upward and downward with vertical versions. This observation shows that extraretinal signals associated with horizontal and vertical versions are part of the computation of visual direction. Hering also observed that a dichoptic afterimage of a cross (a horizontal line in one eye and vertical in the other) retains its perceived shape as the eyes make horizontal vergence eye movements. This important observation shows that extraretinal signals associated with horizontal vergence are not part of the computation of visual direction (Banks, 1995).

Nakayama and Balliet (1977) showed that a line's perceived orientation is affected by torsional eye movements. From this, they concluded that an extraretinal signal exists for torsional movements. They also concluded that the signal's gain is much less than 1. Nakayama and Balliet could not distinguish cyclovergence from cycloversion, so their report does not tell us whether an extraretinal signal for cyclovergence exists. Consequently, we looked for evidence of an extraretinal, cyclovergence signal in the perception of line orientation.

We presented dichoptic afterimages; a horizontal line segment was flashed one-half degree above the fixation point to the left eye and another horizontal segment was flashed one-half degree below fixation to the right eye. This stimulus configuration is identical to the nonius stimulus used in Experiments 1-4 (Figure 5). The afterimage was created by flashing a strobe gun at a distance of 1 m. The afterimage looked like two parallel lines, one above fixation and one below. Two of the three original observers and two new naïve observers participated. After forming the afterimage, the observers verged to a very near distance and then looked up, straight ahead, and down over as large an elevation angle as possible. As they made these movements, they inspected the afterimage to see if the 2 segments remained perceptually parallel.

We know from previous research (eg, Somani et al, 1998) that cyclovergence changes of 2 to 4 degrees should occur for the distances and elevations we used in the afterimage experiment. Thus, if an extraretinal signal exists and has a gain of 1, observers should have seen 2 to 4 degrees changes in the perceived parallelism of the lines as they looked up and down. If there is no such signal, observers should have seen no change in perceived parallelism.

None of the 5 observers detected a change in parallelism. From the nonius settings in Experiments 1-4, we know that observers can detect a deviation from parallelism of less than one-fourth degree. Thus, in terms

of calculating perceived orientation, the afterimage results show that either no extraretinal cyclovergence signal is used or, if one is used, it has a very low gain. This result does not bear directly on the means by which compensation occurs in stereopsis. But along with the failure to observe extraretinal compensation in Experiments 3 and 4, it raises the possibility that there is no extraretinal, cyclovergence signal.

## Reliability of Slant Estimation

To understand how surface slant is estimated by the visual system, we need to consider how different sources of slant information are combined to form a final slant estimate. To do so, we need to consider how errors associated with the measurement of the different sources influence their respective reliabilities and then how the estimates could be combined to yield the most reliable final estimate.

In this paper, we considered stereoscopically defined surfaces slanted about a horizontal axis. We showed that the slant of such surfaces is estimated via measurement of horizontal-shear disparity ($H_R$), vertical-shear disparity ($V_R$), and a distance estimate ($\mu$) that could be determined from an extraretinal signal of horizontal vergence or from the horizontal gradient of vertical disparity (Backus et al, 1999; Rogers & Bradshaw, 1995). We now consider how errors in the measurements of $H_R$, $V_R$, and $\mu$ ought to affect slant estimates based on those signals alone and how those errors ought to affect slant estimates when the surface also provides useful perspective information.

As pointed out earlier, the following equation provides a very accurate estimate of slant from $H_R$, $V_R$, and $\mu$: $S \approx -\tan^{-1}[\frac{1}{\mu}\tan(H_R - V_R)]$. We conducted a Monte Carlo simulation to determine the variance of the slant estimates from this equation (Backus & Banks, 1999). We assumed Gaussian noise (mean = 0) in the measurements of $H_R$, $V_R$, and $\mu$. The assumed standard deviations of the noises for $H_R$, $V_R$, and $\mu$ were 0.132, 0.132, and 0.5 degrees, respectively.[9] With those assumed noises, the estimator would have a slant-discrimination threshold (71% correct) of ~1.5 degrees at a viewing distance of 50 cm and base slant of 0 degree, a threshold value that is consistent with preliminary measurements (Banks, 2000).[10]

In the simulation, the stimulus was always placed in the head's median plane. Viewing distance varied from 20 to 200 cm and slant about the horizontal axis from –70 to 70 degrees.[11] For each viewing condition considered, the simulation drew a value from each signal measurement distribution and calculated a slant estimate. From 20,000 simulation trials, we determined the mean and variance

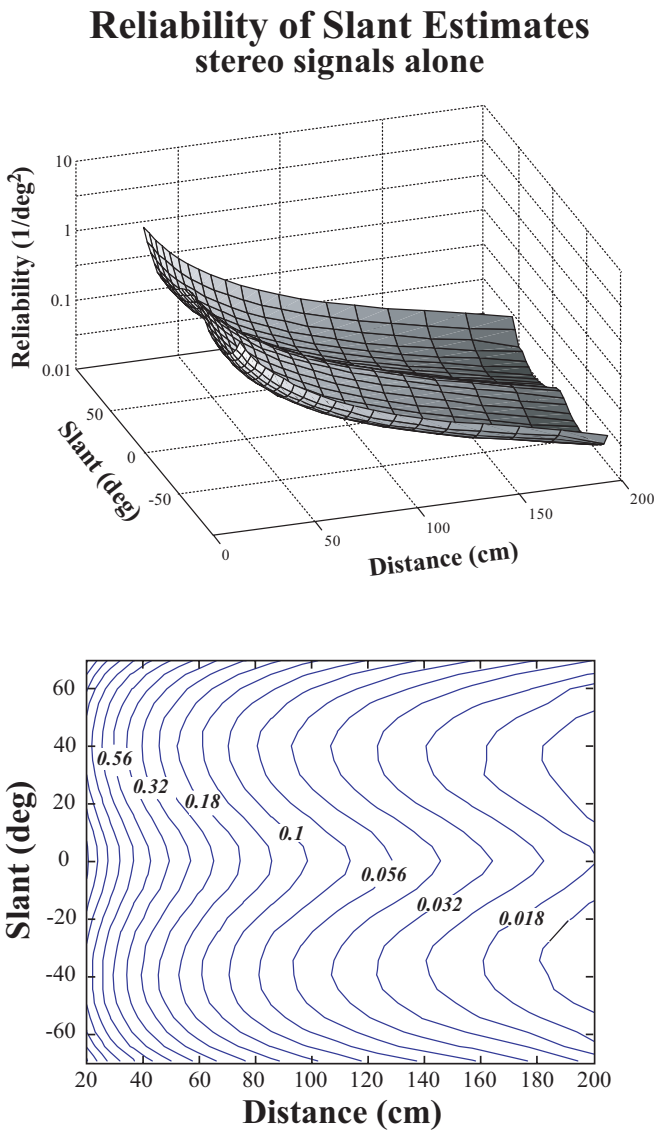


Figure 14. Reliability of slant-from-disparity estimates as a function of distance and slant. The upper panel plots reliability (inverse variance) as a surface plot and the lower panel plots reliability as a contour plot. The labels indicate the reliability associated with each contour. The reliabilities were calculated in a simulation described in the text.

of the distribution of estimates. The means revealed little or no bias (largest biases were ~0.5 degree). Figure 14 shows the reliability (reciprocal of the variance) of the slant estimates. The upper panel is a surface plot and the lower panel a contour plot. The labels in the contour plot indicate the reliability values. There are three discernible effects.[12]

First, as one would expect, the highest reliabilities (lowest estimator variances) are observed at the shortest viewing distances. This occurs because a given change in

disparity gradient corresponds with an increasingly large range of slant as distance increases (Equation 1). Second, there is a ridge of high reliability centered at a slant of 0. This ridge corresponds to viewing conditions in which the horizontal- and vertical-shear disparities are equal to one another ($H_R - V_R = 0$). The reason for the high-reliability ridge can be seen by inspection of Equation 4. When surface slant is ~0, the argument of the tangent is ~0, and, therefore, variance due to error in the measurement of $\mu$ is minimized. Third, ridges of high reliability occur at large slants. This occurs because smaller variations in slant cause increasingly large changes in horizontal-shear disparity as slant increases (the inverse tangent in Equation 4 asymptotes with increasing horizontal-shear disparity).

The distance effect is by far the largest of the three effects. Said another way, reliability does not vary substantially with slant. Based on these simulation results, we hypothesize that stereoscopic slant discrimination (about a horizontal axis) should vary dramatically with distance and minimally with slant.

Slant discrimination based on texture information behaves quite differently. For example, Knill (1998b) has shown that texture-based discrimination thresholds vary dramatically with slant. For the stimuli he used, threshold is ~40 degrees when the base slant is 0 degree and ~2 degrees when the base slant is 70 degrees. From Knill's discrimination data, we can estimate the reliability of the slant-from-texture estimator as a function of slant and distance. We used his data to estimate the variance (and thereby the reliability) of the estimator at different slants. The reliability of the texture estimator should not vary with distance because a surface with a given slant creates precisely the same retinal image at different distances (provided that the surface and its texture are scaled to subtend the same visual angle). The upper panel of Figure 15 plots the resulting estimates of reliability as a function of distance and slant. Reliability is more than a log unit higher when the slant is ±70 degrees than when the slant is 0 degree.

Naturally, texture-based discrimination thresholds will vary depending on several stimulus parameters including field of view, outline shape, and regularity of the texture. Knill's stimuli subtended 20 x 25 degrees, provided no outline shape cue to slant, and consisted of discrete texture elements. The texture elements were ellipses of different sizes and aspect ratios placed at random positions on the surface. With such textures, three cues to slant can be identified (Knill, 1998a): scaling (the spatial distribution of projected texel sizes), foreshortening (the spatial distribution of texel aspect ratios and orientations), and position (the spatial distribution of texel positions). Several investigators have shown that the visual system relies primarily on foreshortening and scaling to estimate slant (Buckley, Frisby, & Blake, 1996; Frisby & Buckley, 1992; Frisby, Buckley, & Freeman, 1996; Knill, 1998b). Those two texture cues provide increasingly reliable slant information as surface slant is increased (Blake, Buelthoff, & Sheinberg, 1993; Knill, 1998a,b). For this reason, one expects that the reliability surface in the upper panel of Figure 15 will move up and down, but remain roughly constant in shape as stimulus parameters such as field of view, texel type, and texel density are varied.

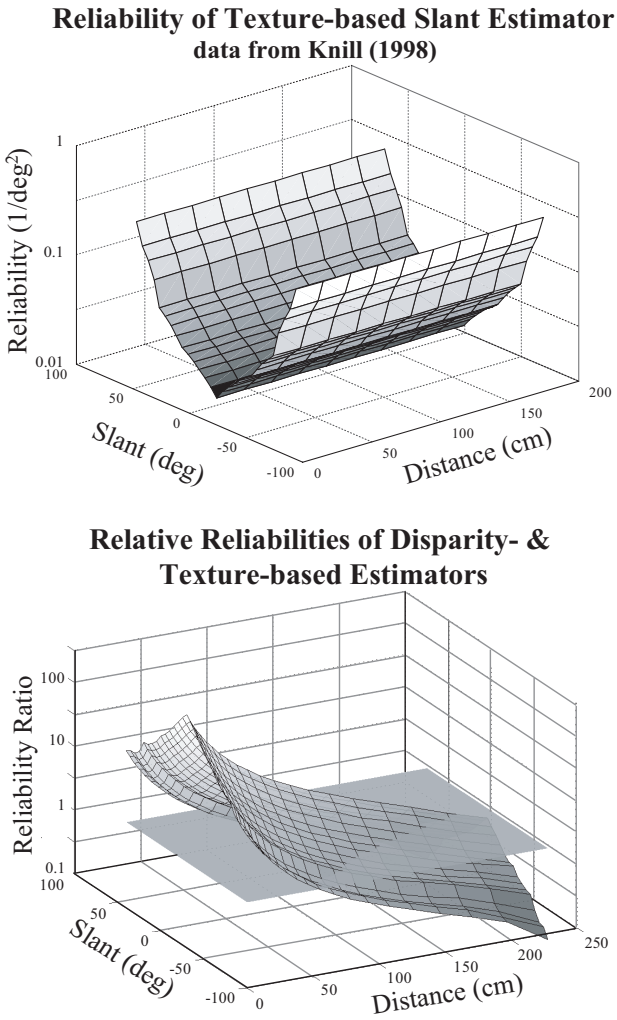


Figure 15. Relative reliabilities of slant-from-texture and slant-from-disparity. The upper panel plots reliability (inverse variance) of slant-from-texture estimates as a function of distance and slant. The reliabilities were calculated from the slant discrimination data of Knill (1998b). The lower panel plots the ratio of reliabilities (disparity/texture) as a function of distance and slant. The slant-from-disparity reliabilities were obtained from Figure 14. The flat gray surface shows the plane for which the reliability ratio is 1.

How should one combine slant-from-disparity and slant-from-texture information when they are both available? If disparity and texture information are statistically independent and Gaussian distributed, the maximum-likelihood estimate of surface slant is given by:

$$\hat{S} = w_d \hat{S}_d + w_t \hat{S}_t \qquad (5)$$

where $\hat{S}_d$ and $\hat{S}_t$ are the disparity and texture estimators (Gharamani, Wolpert, & Jordan, 1997; Landy, Maloney, Johnston, & Young, 1995).

The reliability of an estimator is its inverse variance: $r_d = \frac{1}{\sigma_d^2}$ and $r_t = \frac{1}{\sigma_t^2}$. The weights, $w_d$ and $w_t$, are proportional to the reliabilities:

$$w_d = \frac{r_d}{r_d + r_t}$$

$$w_t = \frac{r_t}{r_d + r_t}.$$

Thus, the weights are directly related to the reliabilities of the estimators and add to 1. Equation 5 shows that the disparity estimator should be given greater weight than the texture estimator when its reliability is higher. To determine the conditions under which this should occur, we calculated the ratio of reliabilities. The lower panel of Figure 15 plots the reliability ratios (disparity/texture) as a function of distance and slant. A reference surface for which the ratio is one is also shown. More weight should be given to the disparity estimator for conditions in which the reliability ratio is above the reference surface. Naturally, the precise form of the relative reliability surface depends on the stimulus used. As we noted above, enriching the slant-from-texture information ought to cause an improvement in texture reliability, which in turn would cause the reliability ratio surface to move downward relative to the reference surface. Similarly, enriching the slant-from-disparity information ought to move the surface upward. The shape of the reliability ratio surface should nonetheless remain roughly constant for the class of stimuli considered here.

The ratio surface shows that the relative reliabilities of the disparity and texture estimators depend on distance and slant.[13] The disparity estimator has greater reliability at short distances and the texture estimator has greater reliability at long distances. However, the point at which the reliabilities are equal occurs at 224 cm when the surface slant is 0 degree, 126 cm when slant is 35 degrees, and 75 cm when slant is 70 degrees. We hypothesize, therefore, that disparity information will be the greater determinant of perceived slant for frontal or nearly frontal surfaces across a broad range of distances. Texture information will be the greater determinant for very slanted surfaces. We are unaware of data that are directly relevant to this hypothesis, but Frisby and Buckley (1992; their Figure 9) reported observations that are consistent with it.

## Influence of Perspective Signals

Numerous investigators have examined the influence of vertical-shear disparity on slant perception (Ogle & Ellerbrock, 1946; Gillam & Rogers, 1991; Howard & Kaneko, 1994; Kaneko & Howard, 1997; Allison et al, 1998; Howard & Pierce, 1998; Pierce et al, 1998; van Ee & Erkelens, 1998), but none has been able to determine the influence quantitatively. Two problems limited their analyses: contamination by monocular slant signals and contamination by the function that maps internal estimates into responses. Here we describe those problems, show how they affect the data, and then explain how we circumvented the problems.

In all but one of the previous studies, the experimenters presented vertical-shear stimuli whose texture gradient and outline shape specified a gaze-normal surface and then asked the observer to indicate the perceived slant by, for example, setting a hand paddle (Gillam & Rogers, 1991; Howard & Kaneko, 1994; Kaneko & Howard, 1997; Howard & Pierce, 1998; Pierce et al, 1998; van Ee & Erkelens, 1998). Figure 4 shows the data from Experiment 2 of Howard and Kaneko (1994). The stimuli were random-dot stereograms in circular windows 10, 30, or 60 degrees in diameter. The gray curve shows the disparity-specified slant (specifically, the predictions of the vertical-disparity-compensation model, Equation 4) and the dashed horizontal line shows the perspective-specified slant. The data for the three stimulus diameters fall between the two predictions, nearer the disparity-specified slant when the diameter was large and nearer the perspective-specified slant when the diameter was small. There are three plausible interpretations of the fact that the data fell short of the disparity-specified prediction.

### *Contamination by the function mapping internal slant estimate into slant response*

In slant-estimation experiments like the ones referred to above, the observer must convert the internal estimate into a response (eg, setting a paddle with the hand to indicate the perceived slant). The experimenter usually does not know the function that maps the internal estimate into the response, so its contribution is generally unknown.[14] This factor would probably not interact with stimulus size, but it could account for the shortfall the three curves have in common.

Table 1. Estimates of eight given to perspective-specified slant

| | Dimensions | Distance | Texture Type | Estimate of $w_p$ |
|---|---|---|---|---|
| Gillam & Rogers (91) | 10 degree square | 90 cm | Random dot | 1.00 |
| Howard & Kaneko (94) | | | | |
| Experiment 1 | 85 x 65 degrees | 61 cm | Random dot | 0.62 |
| Experiment 2 | 60 degree circle | 94 cm | " | 0.44 |
| Experiment 2 | 30 degree circle | " | " | 0.50 |
| Experiment 2 | 10 degree circle | " | " | 0.91 |
| Kaneko & Howard (97) | | | | |
| Experiment 4 | 60 degree circle | 94 cm | Random dot | 0.52 |
| Allison et al. (98) – 30 sec | 60 degree circle | 93 cm | Irregular | 0.52 |
| Howard & Pierce (98) | | | | |
| Experiment 1 | 60 degree square | 89 cm | Various | 0.54 |
| Experiment 2 | 60 degree square | " | " | 0.51 |
| van Ee & Erkelens (98) – 25 sec | 70 degree square | 150 cm | Small circles | 0.55 |

### *Less than full implementation of vertical-disparity compensation*

The nervous system may not fully implement compensation via vertical disparity in the fashion suggested by Equation 4. For example, Howard and Kaneko (1994) interpreted the shortfall in Figure 4 as an inability to fuse stimuli containing vertical-shear disparities greater than ±2 degrees.

### *Contamination by monocular slant signals*

We can model slant-estimation experiments as follows. First, the observer estimates the disparity-specified slant ($\hat{S}_d$; the "hat" indicates a visual estimate rather than the physically specified variable) and the perspective-specified slant ($\hat{S}_p$). The observer then uses a weighted average to determine the best overall slant estimate:

$$\hat{S} = w_d \hat{S}_d + w_p \hat{S}_p ,$$

where $\hat{S}$ is the final slant estimate and the weights ($w_d$ and $w_p$) add to 1 (Landy et al, 1995). For these experiments, ($\hat{S}_p$) = 0, so

$$\hat{S} = (1 - w_p)\hat{S}_d .$$

Thus, whenever the weight given to the perspective-specified slant is greater than 0, the final slant estimate will be less than the disparity-specified slant estimate. The best one can do is to present a stimulus with weak perspective information, such as a very sparse random-dot surface, in the hope of reducing the perspective weight $w_p$ to a small value.

If we assume that the mapping between internal slant estimate and slant response is veridical and that vertical-disparity compensation is fully implemented, we can estimate the weights given the disparity and perspective signals. For the data in Figure 4, the perspective weights are 0.44, 0.50, and 0.91 for diameters of 60, 30, and 10 degrees, respectively. The weights for other previous experiments are given in Table 1. In every case, the perspective weight is greater than 0.43, so the disparity weight is 0.57 or less (again assuming veridical mapping between internal estimate and response).

The inferential problem is that one cannot determine the separate contributions of the three factors listed above. As a consequence, the traditional slant-estimation experiment does not allow one to quantify compensation via vertical disparity (or, for that matter, via eye-position signals).

We circumvented this problem by eliminating the possible contaminating effects of monocular slant signals and of the mapping between estimate and response. This was accomplished by the combined use of a slant-nulling procedure and a stimulus whose perspective-specified slant is always 0 (see "Methods"). Figure 16 shows the data from observer I.T.H. in Experiments 2 and 3. Head-centric horizontal-shear disparity when the stimulus appeared gaze normal is plotted as a function of the head-centric, vertical-shear disparity. The diagonal gray line shows the predicted data if the vertical-disparity compensation suggested by Equation 4 were fully implemented. The circles are the data from Experiment 2 in which the stimulus diameter was 35 degrees and the squares are the data from Experiment 3 in which the stimulus diameter was 5 degrees. Recall that we observed vertical-disparity-based compensation with the larger, but not the smaller, stimulus. The large-diameter data in Figure 16 conform reasonably well to the predictions of the vertical-disparity compensation model. Thus, even with vertical-shear disparities as large as ±4 degrees, the visual system can use the vertical disparity signal effectively to compensate for the presumed eye torsion. This finding is inconsistent with Howard and Kaneko's (1994) explanation for the failure to observe a full effect of vertical disparity.

In conclusion, data obtained using the standard slant-estimation technique reveal that responses fall short of the predictions of the vertical-disparity compensation model. One can argue plausibly that the shortfall is due to some combination of three effects: 1) failure of the visual system to implement vertical-disparity compensation fully, 2) contamination due to the mapping function between internal estimate and response, and 3) intrusion of monocular slant signals. When the contaminating effects are eliminated, we find that vertical-disparity compensation is implemented in a fashion that is close to the model's quantitative predictions.

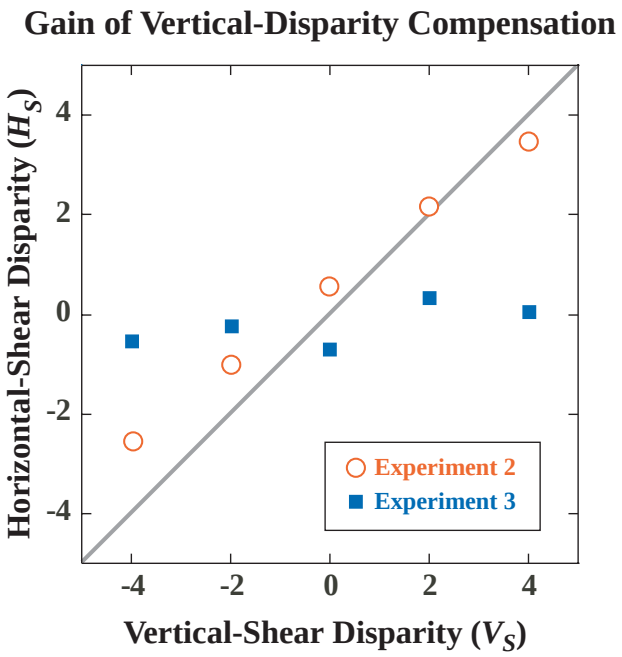


Figure 16. Data from Experiments 2 and 3 plotted as a function of vertical-shear disparity. The head-centric, horizontal-shear disparity that appeared gaze normal is plotted as a function of the head-centric, vertical-shear disparity in the stimulus. The data should fall on the gray diagonal line if veridical compensation based on vertical shear occurs (ie, Equation 4). The circles are the average settings of observer I.T.H. in Experiment 2 (stimulus diameter = 35 degrees). The squares are the average settings of I.T.H. in Experiment 3 (diameter = 5 degrees).

## Ogle and Ellerbrock (1946)

Gillam and Rogers (1991) and Howard and Kaneko (1994) are generally credited with the first demonstration that vertical-shear disparity affects perceived slant.[15] In fact, Ogle and Ellerbrock (1946) demonstrated this 50 years earlier, but have not been credited because they misinterpreted their data. Here we explain their demonstration and how they misinterpreted it.
Ogle and Ellerbrock's observers viewed stimuli through afocal unilateral magnifiers (such lenses magnify the image in one direction only). The lens axis in front of the left eye was 45 degrees and the one in front of the right eye was 135 degrees. Thus, they created the scissors effect (horizontal and vertical shear in opposite directions) illustrated in the upper panel of Figure 17.[16] The stereoscopic stimulus consisted of a thin vertical and thin horizontal line intersecting at the fixation point. When the stimulus was objectively gaze normal, the lenses created a horizontal-shear disparity of $-m$ ($m/2$ and $-m/2$ in the left and right eyes, respectively) and a vertical-shear disparity of $m$. The observer's task was to adjust the slant of the stimulus (about a horizontal axis) until it looked gaze normal. Observers made settings for 10 magnifications (that added vertical-shear disparities of 0.67 to –0.84 degrees).

To understand this experiment, one needs to distinguish the shear disparity at three stages. First, there is the shear disparity created by the stimulus itself. As before, we refer to this head-centric, horizontal disparity as $H_S$. The corresponding vertical-shear disparity is always 0 because rotation of the stimulus about the horizontal axis has no effect on projections of a horizontal line. Second, there are the shear disparities as they leave the lenses and approach the eyes. These head-centric disparities are $H_L$ and $V_L$. If the lenses add a horizontal shear of $m$, then $H_L = H_S + m$ and $V_L = -m$. Finally, the shear disparities at the retina are $H_R$ and $V_R$. These retino-centric values are affected by the eyes' cyclovergence ($\tau$), so $H_R = H_L - \tau$ and $V_R = V_L - \tau$.

Consider what the three slant-estimation models presented here—no compensation, extraretinal compensation, and vertical-disparity compensation—predict for Ogle and Ellerbrock's experiment. We assume that the cyclovergence is driven by the vertical shear at the retina and has a gain of $g$ which has a value between 0 and 1 (Howard & Zacher, 1991). Thus, $\tau = g\, V_R = -gm$.

### No compensation

This means of slant estimation is represented by Equation 2: $S \approx -\tan^{-1}(\frac{1}{\mu}\tan H_R)$ where $H_R$ is the horizontal-shear disparity at the retina and $\mu$ is the vergence distance. $H_R$ is affected by the lenses and the eyes' torsion:

$$H_R = H_L - \tau = (H_S + m) + gm = H_S + (1 + g)m.$$

The observer's task is to adjust the stimulus until $H_R = 0$. Thus, he must alter the horizontal-shear disparity due to the stimulus ($H_S$) in order to undo the shear created by the lenses and eye torsion. Mathematically, this is given by

$$H_S = (1 + g)\, V_L.$$

The left-hand graph in Figure 17 plots predicted slant settings as a function of the added vertical shear ($V_L$). If cyclovergence gain ($g$) is 1, the predicted slant settings are the solid curve. If the gain is 0, the predictions are the dashed curve. The right-hand graph in Figure 17 plots the predicted horizontal-shear disparity approaching the eyes ($H_L$) as a function of the induced vertical-shear disparity ($V_L$). If no compensation for cyclovergence occurs, $H_L = g\, V_L$.

If cyclovergence gain is 1, the predicted slant settings are the solid diagonal line. If the gain is 0, the predictions are the dashed horizontal line.

The filled squares are Ogle and Ellerbrock's data (from their Table 2 and Figure 6). The data are quite consistent with the predictions of the no-compensation model with a cyclovergence gain of 1. In fact, Ogle and Ellerbrock presented this model as an account of their observations. They argued specifically that the induced vertical shear caused cyclovergence which then caused a change in horizontal-shear disparity which in turn affected perceived slant (see also Gillam & Rogers, 1991). Ogle and Ellerbrock concluded that their technique measured cyclovergence and, accordingly, entitled their paper "Cyclofusional movements."

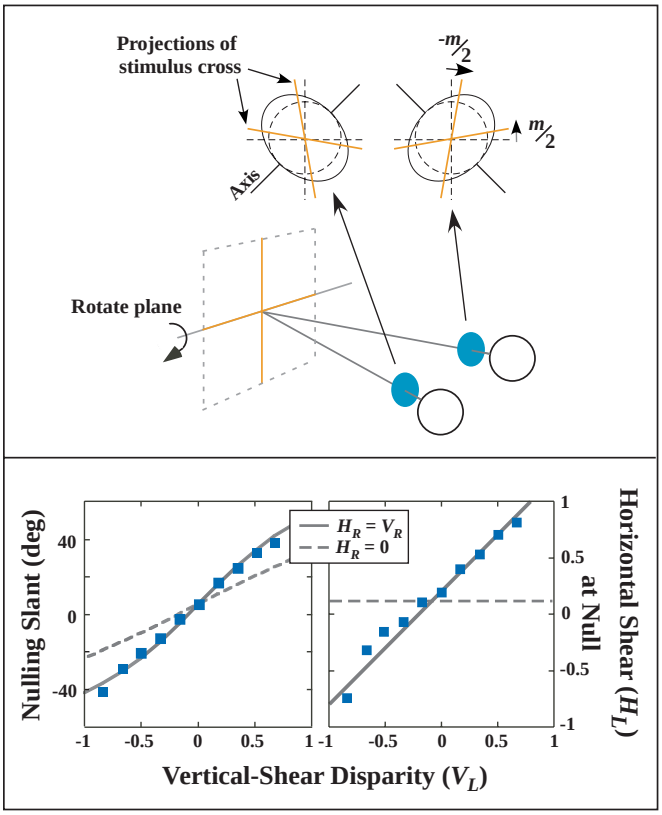


Figure 17. The experiment of Ogle and Ellerbrock (1946). The upper panel depicts the stimulus and the means of manipulating the shear disparities. Observers viewed stimuli through afocal unilateral magnifiers. The lens axes in the two eyes were oblique and orthogonal to one another, so they created the scissors effect illustrated. The stimulus was a cross composed of thin lines. The observers adjusted the slant of the cross (about a horizontal axis) until it appeared gaze normal. Lower left panel: The slants that appeared gaze normal are plotted as a function of the vertical-shear disparity at the corneas ($V_L$). The dashed line represents the predicted settings if there were no cyclovergence (or if cyclovergence occurred along with veridical extraretinal compensation). The solid curve represents the predictions if cyclovergence occurred and the visual system compensated for it veridically by using vertical-shear disparity (Equation 4) or if cyclovergence occurred and the visual system failed to compensate for it. The data points are from Figure 6 and Table 2 in Ogle and Ellerbrock (1946). Lower right panel: The horizontal-shear disparity ($H_L$) approaching the eyes at the slant setting. The dashed line represents the predicted settings if there were no cyclovergence (or extraretinal compensation). The solid diagonal line represents the predictions if cyclovergence occurs and the visual system compensates for it veridically by using vertical-shear disparity (Equation 4) or if cyclovergence occurs and the visual system fails to compensate for it. Again the data points are from Ogle and Ellerbrock.

### *Extraretinal compensation*

This means of slant estimation is represented by Equation 3: $S \approx -\tan^{-1}[\frac{1}{\mu}\tan(H_R + \hat{\tau})]$ where $\hat{\tau}$ is the extraretinal torsion signal (assumed to be accurate: $\tau = \hat{\tau}$) and it is used to correct for the horizontal shear introduced by eye torsion. Again the retinal horizontal-shear disparity ($H_R$) is affected by the lenses and the eyes' torsion, but now the visual system compensates for the part caused by the torsion. Thus, the observer's task is to adjust the stimulus until $H_R + \hat{\tau} = 0$. Because $H_R = H_L - \tau$ and $\tau = \hat{\tau}$, the task becomes:

$$H_L = 0 = H_S + m$$
$$H_S = -m$$
$$H_S = V_L.$$

Therefore, the extraretinal compensation model predicts that the data should lie on the dashed curve in the left part of the figure and on the dashed horizontal line in the right part (because the prediction is $H_L = 0$). Ogle and Ellerbrock's data are clearly inconsistent with these predictions, so we can reject this model. If we assume that the gain of the extraretinal signal (not the gain of the cyclovergence itself) is less than 1, the predictions move in the direction of the solid curve and line; of course, as the extraretinal gain goes to 0, the model becomes the no-compensation model.

### *Vertical-disparity compensation*

This means of estimation is represented by Equation (4): $S \approx -\tan^{-1}[\frac{1}{\mu}\tan(H_R - V_R)]$. $H_R$ is again affected by the lenses and the eyes' torsion, but now the visual system compensates by using the vertical-shear disparity ($V_R$). The observer's task in this model is to set the slant such that the horizontal and vertical-shear disparities at the retina are equal to one another; that is, $H_R - V_R = 0$. We can work out the model's predictions by quantifying the lens and torsion effects on the horizontal and vertical-shear disparities separately. For the horizontal shear,

$$H_R = H_L + gm = (H_S + m) + gm = H_S + (1 + g)m.$$

For the vertical shear,

$$V_R = V_L + gm = (0 - m) + gm = (g - 1)m.$$

Then subtracting $V_R$ from $H_R$ and rearranging,

$$H_S = (g - 1)m - (1 + g)m$$
$$H_S = 2\ V_L.$$

This prediction yields the solid curve in the left-hand part of Figure 17. Similarly, the prediction for the right-hand part of the figure is $H_L = V_L$, which is the solid diagonal line. Ogle and Ellerbrock's data are quite consistent with the predictions of this model. Notice that the predictions do not depend on the gain of the cyclovergence response itself.

We find that Ogle and Ellerbrock's data are consistent with two quite different hypotheses: the no-compensation model and the vertical-disparity compensation model. Which provides a better account? For the no-compensation model to explain the data, the gain of the cyclovergence response must be 1 ($\tau = V_L$). More recent work on cyclovergence reveals that the gain is actually significantly less than 1. Indeed, cyclovergence gains are typically 0.4–0.6 for stimulus conditions like those of the Ogle and Ellerbrock (Howard & Zacher, 1991), so their data almost certainly cannot be explained by the no-compensation model. We conclude that their data manifest the operation of compensation based on vertical-shear disparity and that Ogle and Ellerbrock's data demonstrated a direct effect of vertical-shear disparity on slant perception. They are not credited with the discovery because they did not understand that at the time.

## Estimating Slant About a Horizontal Axis With Eccentric Gaze

The pattern of horizontal disparities on the retinas is affected by the orientation of a surface as well as its position relative to the head. For example, the horizontal size ratio (*HSR*) is affected by slant about a vertical axis as well as the azimuth and distance of the surface from the head (Backus et al, 1999; Ogle, 1950). When the surface is straight ahead (in the head's median plane), *HSR* is 1 when the slant is 0. However, when the surface is 30 degrees to the left of the median plane, *HSR* is 1 when the slant is 30 degrees. To recover the slant of surfaces at different azimuths, the visual system must "correct" the observed *HSR* (Gårding, Porrill, Mayhew, & Frisby, 1995). It does so by using vertical-disparity and eye-muscle signals (Backus et al, 1999).

It has been stated, without proof, that the relationship between slant and horizontal-shear disparity is essentially unaffected by changes in azimuth (Mitchison & McKee, 1990; Mitchison & Westheimer, 1990). If this were true, the estimation of slant about a horizontal axis would not require disparity "correction" for changes in azimuth. Here we evaluate this hypothesis quantitatively.

Figure 18 shows the geometry of the viewing situation. A vertical line (*V*) is positioned in the head's median plane at distance *d*. The stimulus is a surface rotated about the horizontal axis through the fixation point (*F*). *P* lies on this surface and in the head's median plane. The head is rotated about a vertical axis through

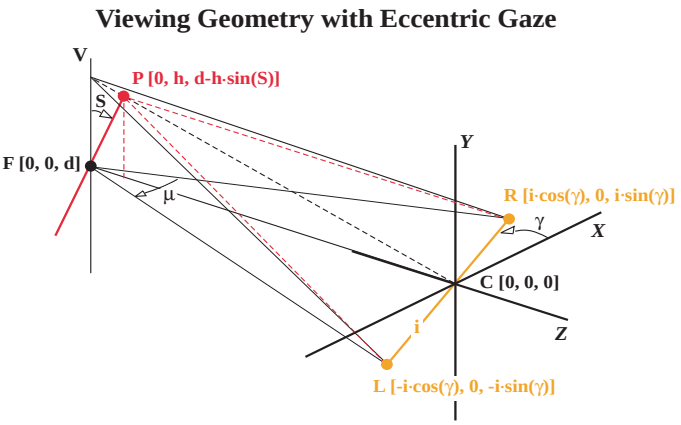


Figure 18. Binocular viewing geometry with eccentric gaze. The midpoint between the eyes (*C*) is the origin of the coordinates. The eyes are separated by *2i* and the head is rotated about a vertical axis through the angle γ. The eyes are fixating a point *F* on the vertical line *V* at distance *d*. The vertical line is then slanted about a horizontal axis by angle *S* so that the top is closer to the observer. *P* on the slanted line is in the head's median plane. The horizontal-shear disparity created by this slanted line is then calculated. The eyes' vergence is μ.

the angle γ. The eyes' vergence (μ) is the angle subtended by the lines of sight at *F*. We calculated the horizontal-shear disparity ($H_R$) by using standard cameras positioned at the left and right eyes and pointed at *F*. We examined how two means of slant estimation—the ones expressed by Equations 1 and 4—are affected by head rotation:

$$S = -\tan^{-1}\left[\frac{\tan(H_R/2)}{\sin(\tan^{-1}(i/2d))}\right] \qquad (1)$$

$$S \approx -\tan^{-1}\left[\frac{1}{\mu}\tan(H_R - V_R)\right]. \qquad (4)$$

There are two geometric effects of rotating the head. First, the image becomes larger in the eye that is closer to the stimulus and smaller in the eye that is farther from the stimulus. This has no effect on the horizontal-shear disparity, as we have defined it, because overall magnification does not affect orientation, so the accuracy of Equations 1 and 4 is unaffected by the magnification. Second, the effective baseline between the two eyes decreases as the head rotates from the frontal position. Equation 1 uses a ratio of interocular distance and stimulus distance to "normalize" the disparities for such baseline changes and Equation 4 uses vergence (μ) for the same purpose. The use of vergence is preferable because it compensates for the baseline change with eccentric viewing.

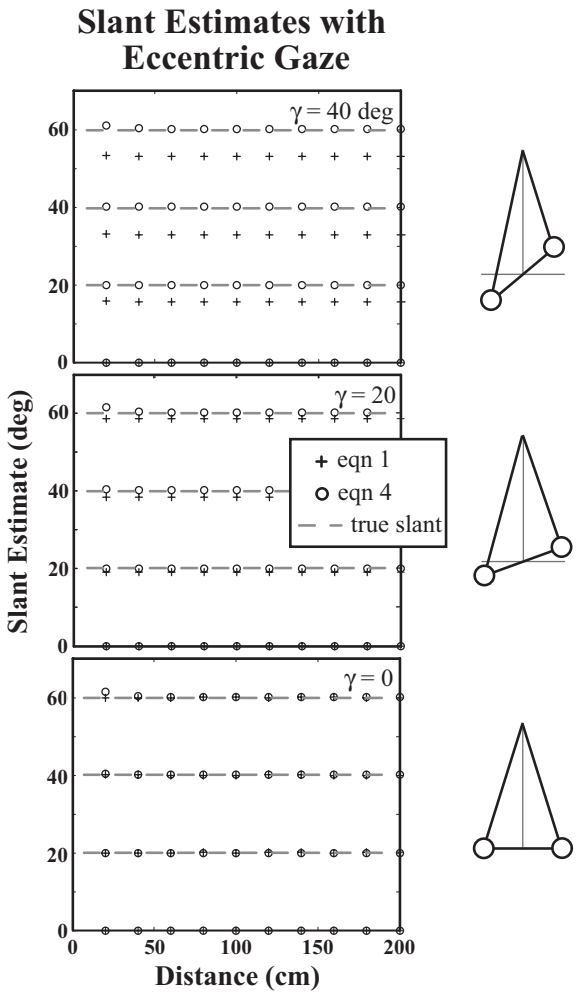


Figure 19. Slant estimates as a function of slant and distance. The upper, middle, and lower panels show the estimates when the head rotation is 40, 20, and 0 degrees, respectively. The icons on the right depict each of those rotations. The panels plot the slant estimate as a function of distance. The true slants are represented by the orange dashed lines. Estimates based on Equation 1 are represented by the crosses and estimates based on Equation 4 by the small circles.

Each panel of Figure 19 plots the slant estimate as a function of distance. The upper, middle, and lower panels show the results when the head rotation is 40, 20, and 0 degrees, respectively. The true slants are represented by the dashed lines and the estimates from Equations 1 and 4 by the crosses and circles, respectively. Equation 1 is an exact expression when γ = 0, but it underestimates slant as the head is rotated through larger angles. As expected, Equation 4 provides a much more accurate estimate of slant when the head is rotated; the largest error is ~2 degrees when the true slant is 60 degrees and the distance is 20 cm. Thus, slant about a horizontal axis can indeed be measured quite accurately without taking gaze azimuth into account. Obviously, horizontal-axis slant can also be measured accurately by Equation 4 when the observer looks up and down

because cyclovergence that occurs with changes in gaze elevation is taken into account by using the induced vertical-shear disparity. Many investigators have observed an anisotropy in stereoscopic slant perception (eg, Buckley & Frisby, 1993; Cagenello & Rogers, 1993; Rogers & Graham, 1983; Wallach & Bacon, 1976; Mitchison & McKee, 1990): for a given physically specified slant, more slant is perceived when the stimulus is rotated about a horizontal axis than when it is rotated about a vertical axis.

What might be the cause of slant anisotropy? The estimation of slant about vertical and horizontal axes is in some ways equivalent. In both cases, the visual system needs to measure horizontal disparities; for vertical-axis slant, it measures horizontal size disparity (*HSR*) and for horizontal-axis slant, it measures horizontal shear disparity ($H_R$). Furthermore, in both cases, the system must "normalize" the disparities with a distance estimate. In some respects, however, vertical-axis slant estimation differs from horizontal-axis estimation. Changes in stimulus azimuth have a profound effect on the relationship between horizontal disparity and vertical-axis slant and, as we have shown here, none on the relationship between horizontal disparity and horizontal-axis slant. In contrast, changes in cyclovergence affect the relationship between horizontal disparity and horizontal-axis slant (Figure 3) and presumably do not affect the relationship between horizontal disparity and vertical-axis slant. The visual system must "correct" the disparities with an estimate of gaze azimuth in the vertical-axis case and with an estimate of cyclovergence in the horizontal case. Gaze azimuth varies substantially during natural viewing: human observers frequently adopt eye positions that are 20 degrees left or right of the median plane. Cyclovergence, on the other hand, does not vary substantially in natural viewing: as discussed earlier, a consequence of Listing's Extended Law is that the eyes remain torsionally aligned (or nearly so) as an observer looks at a near target. The requirement for disparity correction is, therefore, generally greater in vertical- than in horizontal-axis estimation. As a consequence, the visual system may place greater reliance on stereoscopic slant estimation in the horizontal-axis case.

This argument is similar to one made by Mitchison and Westheimer (1990) and Mitchison and McKee (1990). They argued that the requirement for taking eye position into account is greater for vertical- than for horizontal-axis slant and, consequently, there is greater uncertainty in the estimate of vertical-axis slant. Our quantitative analysis is consistent with this idea.

## Acknowledgments

This work was supported by research grants from the Air Force Office of Scientific Research and National Science Foundation (F49620-98), Human Frontiers of Science (RG-34/96), and NSF (DBS-9309820). We thank Mike Landy, Suzanne McKee, and Cliff Schor for comments on an earlier draft. We thank Dave Rehder and Nick Lines for their work in designing and constructing the haploscope, Marc Ernst for assisting with the construction of Figure 1 and Sergei Gepshtein for assisting with the statistical analysis.

## Footnotes

[1] Equation 1 can be derived analytically. Impose a coordinate system on the head such that the x-axis is the interocular axis, y is straight up and down, and $z$ is forward and back. Then the eyes are at $(\pm i/2, 0, 0)$ and a fixation point $F$ is at $(0, 0, z)$. A plane goes through $F$ and a line parallel to the x-axis. Line $L$ is within that plane and within the head's median plane; the line also contains $F$. $L$ has slant $S$ (the angle between $L$ and the y-axis). $H_R$ can then be written in terms of $S$, $i$, and $d$ by considering the projection of $L$ onto image planes at the eyes (ie, planes that are normal to lines of sight from each eye to $F$, respectively): $H_R$ is the difference in the deviation of these projected lines from the vertical. Ogle and Ellerbrock (1946) presented the following equation for estimating slant from horizontal-shear disparity:

$$S \approx \tan^{-1}\left(\frac{d}{i}\tan H_R\right).$$

This same expression reappears in van Ee and Erkelens (1996). Equation 2 is slightly more accurate than Ogle and Ellerbrock's equation when the surface is in the head's median plane and, as we show in the discussion, it is much more accurate than Equation 1 and Ogle and Ellerbrock's equation when the surface is to either side of this plane.

[2] We use right-hand coordinates, so the sign conventions are the following. For positive $H_R$ (and $V_R$), the right-eye's image is rotated clockwise relative to the left eye's. For positive $\tau$, the right eye is rotated clockwise relative to the left eye. For positive $S$, the surface is slanted top toward the observer.

[3] Nakayama and Balliet (1977) have presented circumstantial evidence for an extraretinal signal for the cyclo*version* state of the eyes, but to our knowledge, there is no evidence for an extraretinal signal for the cyclo*vergence* state.

[4] Because the lines of sight are perpendicular to both CRTs, the orientation difference at the eyes is given by the orientation difference in the calibration planes just in front of the CRTs (Backus et al, 1999).

[5] Our procedure for eliminating intrusion due to monocular slant signals would not achieve the desired result if observers perceived a non-zero slant from the monocular signals alone. As a check against the possibility, Backus et al (1999) conducted a monocular control experiment. Stimuli like those in this paper were

presented and observers made slant-nulling settings. The standard deviations of the settings were generally 10 times greater than when the task was performed binocularly. Thus, perceived slant from monocular signals was ill-defined and could have had little effect on slant settings in the binocular experiments. Admittedly, the task in Backus et al was different because it involved slant about a vertical axis, but there is no reason to believe that monocular signals are more informative for slant about a horizontal axis (eg, Buckley & Frisby, 1993). Thus, we are confident that monocular slant signals had no discernible effect on the data in the present report.

[6] By using 100-msec flashes, we could be sure that the stimulus did not cause a change in cyclovergence before it disappeared.

[7] We averaged across the settings for a given value of the conditioning stimulus.

[8] Kaneko and Howard (1997) did an experiment that was designed to reveal whether an extraretinal, cyclovergence signal affects perceived slant. In their fourth experiment, they adapted observers to displays with different amounts of cyclodisparity and then flashed planar stimuli in order to determine whether the adaptation affected subsequent percepts. They found no effect and concluded that the visual system does not use an extraretinal cyclovergence signal in slant estimation. This conclusion, however, is not warranted because they could not rule out the possibility that compensation due to vertical-shear disparity overrode an extraretinal-based compensation.

[9] We assumed that the standard deviations for $H_R$ and $V_R$ were equal. We assumed that the standard deviation for $\mu$ was 0.5 deg because that value seems reasonable and because we used it in a previous paper (Backus & Banks, 1999). We then found the values of $H_R$ and $V_R$ that yielded the desired slant-discrimination threshold of ~1.5 deg at 50 cm.

[10] We assumed fixed Gaussian noise with identical standard deviations for $H_R$ and $V_R$. This assumption would be falsified by an observation that the measurement of $H_R$ or $V_R$ is more accurate for some values than others. The measurement of $H_R$ and $V_R$ would be less accurate if the disparities approached or exceeded the fusion range, but with small surfaces straddling the fixation point, the disparities remain small and fusable, so our assumption seems reasonable for the estimation of local slant near the fixation point. We also assumed that the standard deviations associated with $H_R$ and $V_R$ measurements are the same, but one might argue that the measurement of $V_R$ is more accurate because the visual system seems to measure it over a large portion of the available stimulus (Stenton, Frisby, & Mayhew, 1984). In Equation 4, however, the argument of the tangent is $H_R - V_R$, so the effect on the slant estimate is the same for various combinations of errors in $H_R$ and $V_R$ as long as their variances add to a constant. The assumption that the vergence measurement is Gaussian distributed is presumably false because a sensible system would not accept vergence estimates less than 0. Fortunately, given the relatively short distances used in the simulation and the small vergence error, such estimates were extremely uncommon in the simulation, so again this assumption is reasonable for our purposes.

[11] Variations in cyclovergence had no effect on the simulation. The reason is obvious from Equation 4. Changes in cyclovergence have the same effect on $H_R$ and $V_R$, so it has no effect on the difference.

[12] We explored how the choice of standard deviations for the $H_R$, $V_R$, and $\mu$ noises affected the outcome of the simulation. Changing the values by a factor of two had little effect. However by making larger changes, two discernible effects could be observed. When $\mu$ noise was large and $H_R$ and $V_R$ noises small, the high-reliability ridges at large slants diminished, leaving a single ridge in the middle. When the $H_R$ and $V_R$ noises were large and $\mu$ noise was small, the reliability ridge in the middle of the panels diminished, leaving a wide valley with ridges on the sides.

[13] The fact that the weight given a slant estimator ought to be a function of the slant it is trying to estimate seems odd. There is no logical problem, however, because the slant-from-disparity and slant-from-texture estimators could provide separate slant estimates before the weights are assigned. Then the estimator that combines the two could assign weights based on those estimates.

[14] Howard and Kaneko (1994) and Kaneko and Howard (1997) circumvented this problem to some degree by using the results from a control experiment to normalize their data. In the control experiment, observers used the slant-estimation procedure while viewing a real, full-cue surface. Howard and Kaneko then used those data to scale the observers' responses in their main experiments.

[15] Porrill, Mayhew, & Frisby (1989) stated that they too observed a "vertical shear induced effect."

[16] The transformation can be quantified as a deformation as well (Gillam & Rogers, 1991; Koenderink & van Doorn, 1976).

## References

Allison, R. S., Howard, I. P., Rogers, B. J., & Bridge, H. (1998). Temporal aspects of slant and inclination perception. *Perception, 27,* 1287-1304. [PubMed]

Backus, B. T., & Banks, M. S. (1999). Estimator reliability and distance scaling in stereoscopic slant perception. *Perception, 28,* 217-242. [PubMed]

Backus, B. T., Banks, M. S., van Ee, R., & Crowell, J. A. (1999). Horizontal and vertical disparity, eye position, and stereoscopic slant perception. *Vision Research, 39,* 1143-1170. [PubMed]

Banks, M. S. (1995). *The optometer's sketchpad: Binocular vision and space perception.* Berkeley: Key Curriculum Press.

Banks, M. S. (2000). Stereoscopic contrast illusions. *Investigative Ophthalmology and Visual Science*, Suppl. 41, 949.

Banks, M. S., & Backus, B. T. (1998). Extra-retinal and perspective cues cause the small range of the induced effect. *Vision Research, 38,* 187-194. [PubMed]

Blake, A., Buelthoff, H. H., & Sheinberg, D. (1993). Shape from texture: ideal observers and human psychophysics. *Vision Research, 33,* 1723-1737. [PubMed]

Buckley, D., & Frisby, J. P. (1993). Interaction of stereo, texture and outline cues in the shape perception of three-dimensional ridges. *Vision Research, 33,* 919-933. [PubMed]

Buckley, D., Frisby, J. P., & Blake, A. (1996). Does the human visual system implement an ideal observer theory of slant from texture? *Vision Research, 36,* 1163-1176. [PubMed]

Cagenello, R., & Rogers, B. R. (1993). Anisotropies in the perception of stereoscopic surfaces: The role of orientation disparity. *Vision Research, 33,* 2189-2201. [PubMed]

Frisby, J. P., & Buckley, D. (1992). Experiments on stereo and texture cue combination in human vision using quasi-natural viewing. In G. A. Orban and H. H. Nagel (Eds.), *Artificial and biological visual systems.* Berlin: Springer.

Frisby, J. P., Buckley, D., & Freeman, J. (1996). Stereo and texture cue integration in the perception of planar and curved large real surfaces. In T. Inui and J. L. McClelland (Eds.), *Perception and communication*. Hillsdale, N.J.: Erlbaum.

Gårding, J., Porrill, J., Mayhew, J. E. W., & Frisby, J. P. (1995). Stereopsis, vertical disparity and relief transformations. *Vision Research, 35,* 703-722. [PubMed]

Gharamani, Z., Wolpert, D. M., & Jordan, M. I. (1997). Computational models of sensorimotor integration. In P. G. Morasso and V. Sanguineti (Eds.), *Self-organization, computational maps, and motor control.* Amsterdam: North-Holland.

Gibson, J. J. (1950). *The perception of the visual world.* Boston: Houghton Mifflin.

Gillam, B., & Lawergren, B. (1983). The induced effect, vertical disparity, and stereoscopic theory. *Perception and Psychophysics, 34,* 121-130. [PubMed]

Gillam, B., & Rogers, B. J. (1991). Orientation disparity, deformation, and stereoscopic slant perception. *Perception and Psychophysics, 20,* 441-448. [PubMed]

Hering, E. (1868). *Die Lehre vom Binocularen Sehen.* Leipzig: Engelmann.

Hillis, J. M., & Banks, M. S. (2001). Are corresponding points fixed? *Vision Research, 41,* 2457-2473. [PubMed]

Hooge, I. T. C., Banks, M. S., & van den Berg, A. V. (2001). The dual coil and nonius setting technique for measuring static cyclovergence compared. *Vision Research*, submitted.

Howard, I. P., & Kaneko, H. (1994). Relative shear disparities and the perception of surface inclination. *Vision Research, 34,* 2505-2517. [PubMed]

Howard, I. P., Ohmi, M., & Sun, L. (1993). Cyclovergence: A comparison of objective and psychophysical measurements. *Experimental Brain Research, 97,* 349-355. [PubMed]

Howard, I. P., & Pierce, B. J. (1998). Types of shear disparity and the perception of surface inclination. *Perception, 27,* 129-145. [PubMed]

Howard, I. P., & Rogers, B. J. (1995). *Binocular vision and stereopsis.* Oxford: Oxford University Press.

Howard, I. P., & Zacher, J. E. (1991). Human cyclovergence as a function of stimulus frequency and amplitude. *Experimental Brain Research, 97,* 445-450. [PubMed}

Kaneko, H., & Howard, I. P. (1997). Spatial properties of shear disparity processing. *Vision Research, 37,* 315-323. [PubMed]

Knill, D. C. (1998a). Surface orientation from texture: ideal observers, generic observers and the information content of texture cues. *Vision Research, 38,* 1655-1682. [PubMed]

Knill, D. C. (1998b). Discrimination of planar surface slant from texture: human and ideal observers compared. *Vision Research, 38,* 1683-1711. [PubMed]

Koenderink, J. J., & van Doorn, A. J. (1976). Geometry of binocular vision and a model for stereopsis. *Biological Cybernetics, 21,* 29-35. [PubMed]

Landy, M. S., Maloney, L. T., Johnston, E. B., & Young, M. (1995). Measurement and modeling of depth cue combination: in defense of weak fusion. *Vision Research, 35,* 389-412. [PubMed]

Mitchison, G. J., & McKee, S. P. (1990). Mechanisms underlying the anisotropy of stereoscopic tilt perception. *Vision Research, 30,* 1781-1791. [PubMed]

Mitchison, G. J., & Westheimer, G. (1990). Viewing geometry and gradients of horizontal disparity. In C. Blakemore (Ed.),*Vision: coding and efficiency.* Cambridge: Cambridge University Press.

Nakayama, K., & Balliet, R. (1977). Listing's law, eye position sense, and perception of the vertical. *Vision Research, 17,* 453-457. [PubMed]

Ogle, K. N. (1950). *Researches in binocular vision.* New York: Hafner.

Ogle, K. N., & Ellerbrock, V. J. (1946). Cyclofusional movements. *AMA Archives of Ophthalmology, 36,* 700-735.

Pierce, B. J., Howard, I. P., & Feresin, C. (1998). Depth interactions between inclined and slanted surfaces in vertical and horizontal orientations. *Perception, 27,* 87-103. [PubMed]

Porrill, J., Mayhew, J.E.W., & Frisby, J.P. (1989). Cyclotorsion, conformal invariance, and induced effects in stereoscopic vision. In S. Ullman (Ed.), *Image understanding.* Norwood, N.J.: Ablex Publishing.

Rogers, B. J. (1992). The perception and representation of depth and slant in stereoscopic surfaces. In G. A. Orban and H. H. Nagel (Eds.), *Artificial and biological vision systems.* Berlin: Springer.

Rogers, B. J., & Bradshaw, M. F. (1995). Disparity scaling and the perception of frontoparallel surfaces. *Perception, 24,* 155-179. [PubMed]

Rogers, B. J., & Bradshaw, M. F. (1993). Vertical disparities, differential perspective and binocular stereopsis. *Nature, 361,* 253-255. [PubMed]

Rogers, B. J., & Graham, M. E. (1983). Anisotropies in the perception of three-dimensional surfaces. *Science, 221,* 1409-1411. [PubMed]

Somani, R. A., DeSouza, J. F., Tweed, D., & Vilis, T. (1998). Visual test of Listing's law during vergence. *Vision Research, 38,* 911-923. [PubMed]

Stenton, S. P., Frisby, J. P., & Mayhew, J. E. W. (1984). Vertical disparity pooling and the induced effect. *Nature, 309,* 622-624. [PubMed]

Tweed, D. (1997). Visual-motor optimization in binocular control. *Vision Research, 37,* 1939-1951. [PubMed]

van Ee, R., & Erkelens, C. J. (1996). Stability of binocular depth perception with moving head and eyes. *Vision Research, 36,* 3827-3842. [PubMed]

van Ee, R., & Erkelens, C. J. (1998). Temporal aspects of stereoscopic slant estimation: an evaluation and extension of Howard and Kaneko's theory. *Vision Research, 38,* 3871-3882. [PubMed]

Wallach, H., & Bacon, J. (1976). Two forms of retinal disparity. *Perception and Psychophysics, 19,* 375-382.